

THESIS FOR THE DEGREE OF DOCTOR OF PHILOSOPHY IN NATURAL SCIENCE,  
SPECIALIZATION IN CHEMISTRY

**Alkali Metals and Tar in Biomass  
Thermochemical Conversion:  
Development and Application of Online  
Measurement Techniques**

Dan Gall



**UNIVERSITY OF GOTHENBURG**

Department of Chemistry and Molecular Biology  
University of Gothenburg  
SE-412 96 Gothenburg  
Sweden

Doctoral thesis submitted for fulfilment of the requirements for the degree of  
Doctor of Philosophy in Chemistry

Alkali Metals and Tar in Biomass Thermochemical Conversion:  
Development and Application of Online Measurement Techniques  
© Dan Gall, 2018

Atmospheric science,  
Department of Chemistry and Molecular Biology,  
University of Gothenburg,  
SE-412 96 Gothenburg,  
Sweden

Printed by BrandFactory AB  
Källered, Sweden

ISBN: 978-91-629-0460-9 (print)  
ISBN: 978-91-629-0461-6 (pdf)  
<http://hdl.handle.net/2077/54937>

## Abstract

---

Biomass is a renewable resource that can substitute the fossil-based products we depend on today. However, the conversion techniques require further improvement in order to be competitive with the traditional industry. One of the limitations is associated with the absence of measurement methods with sufficient time resolution that can be used to characterize the complex systems and optimize process conditions.

This thesis presents the development and application of novel measurement methods, capable of time-resolved characterization of tar and alkali metals, which are key components in biomass gasification. The measurement methods are mainly adapted from aerosol science and based on thermal analysis and surface ionization of aerosol particles. Long-term measurements are achieved by dilution and conditioning of hot product gas, which allow condensable components to form aerosol particles that are subsequently analyzed.

The developed methods are used to determine alkali, tar and particle concentrations in industrial scale facilities for biomass gasification. The aerosol characterization methods are also applied in flame chemistry and radiation research. Studies performed in dual-fluidized bed (DFB) gasification systems indicate that the alkali metal content of biomass to a large extent is emitted during the gasification process, and observed concentrations are close to the levels predicted by equilibrium calculations. The high alkali concentrations have implications for catalytic processes in the fluidized beds and for downstream processes including corrosion, fouling, and upgrading to commercial products.

The developed methods are employed to characterize the transient conditions when changes in operational parameters and additives are used to optimize the gasification process. A significant increase of the alkali metal concentration was observed when alkali salts were inserted directly to a gasifier, which suggests a fast volatilization in the reducing environment. Additives to the combustion side of the DFB imposed notable effects in the product gas, and the results provide information regarding the transfer mechanisms of inorganic compounds in the system. Additions of olivine and ilmenite reduced the gas-phase alkali metal concentration, indicating a fast reaction between alkali metal compounds and the minerals. The applied changes also affected the formation of condensable tar, and the tar concentration was found to anti-correlate with the alkali metal concentration when a sand bed was used, while no clear trend was observed with an olivine bed.

The studies confirm that several options are available to improve the alkali metal and tar behavior in biomass gasification, and suggest that online monitoring is needed to study and optimize the underlying processes.

**Keywords:** Tar, Alkali Metals, Biomass, Thermochemical conversion, Online Measurements.

## Abstrakt

---

Biomassa är en förnyelsebar energikälla som kan ersätta de fossila produkter som vi är beroende av idag. Teknikerna för att omvandla det fasta materialet till gas kräver emellertid ytterligare utveckling för att vara konkurrenskraftiga med den traditionella industrin. En av begränsningarna är kopplad till bristen på mätmetoder som med tillräcklig tidsupplösning kan karakterisera de komplexa systemen och optimera processförhållandena.

Denna avhandling presenterar utveckling och tillämpning av nya mätmetoder, kapabla till tidsbestämd karakterisering av tjära och alkalimetaller, vilka är nyckelkomponenter vid förgasning av biomassa. Mätmetoderna baseras på termisk analys och ytjonisering av aerosolpartiklar och har anpassats från aerosolvetenskap. Långa mätserier möjliggjordes genom spädning och konditionering av het produktgas, vilket resulterar i att kondenserbara komponenter bildar aerosolpartiklar som därefter analyseras.

De utvecklade metoderna används för att bestämma alkali-, tjär- och partikelkoncentrationer i anläggningar av industriella skala för förgasning av biomassa. Aerosol karakteriseringsmetoderna tillämpas också i flamm- och strålningsforskning. Studier utförda i förgasningssystem med dubbel fluidiserad bädd (DFB) indikerar att alkalimetallinnehållet i biomassa i stor utsträckning emitteras under förgasningsprocessen och observerade koncentrationer ligger nära de nivåer som förutses av jämviktsberäkningar. De höga alkalimetallkoncentrationerna har implikationer för katalytiska processer i de fluidiserade bäddarna samt för nedströms processer innefattande korrosion, beläggning och uppgradering till kommersiella produkter.

De utvecklade metoderna används för att karakterisera transienta förhållanden i samband med förändringar av driftsparametrar och tillsatser som används för att optimera förgasningsprocessen. En signifikant ökning av alkalimetallkoncentrationen observerades när alkalialter tillsattes direkt till en förgasare, vilket indikerar en hastig förångning i den reducerande miljön. Additiver till förbränningssidan av DFB medförde märkbara effekter i produktgasen, och resultaten bidrar med information om överföringsmekanismerna för oorganiska föreningar i systemet. Tillsatser av olivin och ilmenit reducerade gasfas-alkalimetallkoncentrationen, vilket indikerar på en snabb reaktion mellan alkalimetallföreningar och mineralerna. De utförda förändringarna påverkar också bildandet av tyngre tjäror och tjärkoncentrationen visade sig korrelera med alkalimetallkoncentrationen när en sandbädd användes, medan ingen tydlig trend observerades med en olivinbädd.

Studierna bekräftar att flera alternativ är tillgängliga för att förbättra alkalimetall- och tjärbehandlingen vid förgasning av biomassa och visar att online-mätningar behövs för att studera och optimera de underliggande processerna.

## List of publications

---

- I. **Online Measurements of Alkali and Heavy Tar Components in Biomass Gasification.** Dan Gall, Mohit Pushp, Kent O. Davidsson, Jan B. C. Pettersson. *Energy & Fuels*, 2017, 31, 8152-8161.
- II. **Online Measurements of Alkali Metals during Start-up and Operation of an Industrial-Scale Biomass Gasification Plant.** Dan Gall, Mohit Pushp, Anton Larsson, Kent O. Davidsson, Jan B. C. Pettersson. *Energy & Fuels*, 2018, 32, 532-541.
- III. **Influence of fluidized bed material and operational conditions on alkali metal and heavy tar concentrations in biomass gasification.** Mohit Pushp, Dan Gall, Kent Davidsson, Martin Seemann, Jan B. C. Pettersson. Submitted to *Energy & Fuels*.
- IV. **Particle composition and size distribution in coal flames – The influence on radiative heat transfer.** Daniel Bäckström, Dan Gall, Mohit Pushp, Robert Johansson, Klas Andersson, Jan B.C. Pettersson. *Experimental Thermal and Fluid Science*, 2015, 64, 70–80.
- V. **A Novel Field Reversal - Surface Ionization Method for Characterization of Biomass Burning and Sea Salt Aerosols.** Dan Gall, Charlotta Nejman, and Jan B. C. Pettersson. Manuscript for *Atmospheric Measurement Techniques*.

## Statement of contribution

---

- I. Dan Gall is the main author together with Jan Pettersson, and was responsible for conducting the experiment and evaluating the results.
- II. Dan Gall is the main author together with Jan Pettersson. Dan Gall and Mohit Pushp conducted the experimental work and evaluated the results.
- III. Dan Gall is one of the main authors together with Mohit Pushp and Jan Pettersson. The experiment were conducted by Dan Gall together with Mohit Pushp. Data evaluation was mainly performed by Jan Pettersson and Dan Gall.
- IV. Daniel Bäckström is the main author of this work. Dan Gall conducted and evaluated the particle measurements.
- V. Dan Gall is the main author together with Jan Pettersson. Charlotta Nejman conducted and evaluated part of the experiments during her Master thesis project supervised by Jan Pettersson and Dan Gall.

## Contents

Abstract.....	ii
List of publications .....	iv
Statement of contribution.....	v
List of Abbreviations.....	viii
1. Introduction.....	1
2. Background .....	3
2.1 Utilizing biomass.....	3
2.2 Biomass gasification.....	3
2.3 Tar measurements .....	5
2.3.1 Classification of tar.....	5
2.3.2 Tar measurement techniques.....	6
2.4 Alkali metal measurements.....	7
2.4.1 Alkali metal release during gasification.....	7
2.4.2 Alkali measurements in biomass gasification .....	8
2.5 Alkali metals in DFB gasification.....	10
3. Experimental techniques .....	12
3.1 Controlled nucleation .....	12
3.2 Aerosol characterization techniques.....	16
3.2.1 Scanning Mobility Particle Sizer (SMPS).....	16
3.2.2 Optical aerosol spectrometer .....	18
3.3 Thermal stability analysis.....	19
3.3.1 Volatility Tandem DMA (VTDMA).....	20
3.4 Surface ionization technique.....	23
3.4.1 Surface ionization detector (SID).....	24
3.4.2 Field Reversal – SID (FR-SID).....	25
3.5 Evaluation and calibration .....	26
3.5.1 Measurement uncertainty .....	27

4. Industrial facilities.....	29
4.1 The Chalmers Gasifier .....	29
4.2 The Gothenburg Bio-Gas facility.....	30
4.3 Chalmers oxy-fuel test rig .....	31
5. Results and discussion.....	32
5.1 Laboratory studies.....	32
5.1.1 Volatility measurements.....	32
5.1.2 FR-SID development.....	34
5.2 Field results .....	36
5.2.1 Thermal stability of particles from gasification and combustion processes .....	36
5.2.2 Effects of indirect additives.....	38
5.2.3 Effect of additives directly to the gasifier .....	41
5.3 Alkali metal and tar chemistry .....	42
6. Conclusions .....	44
Acknowledgement .....	46
References.....	49

## List of Abbreviations

---

BFB -	Bubbling Fluidized Bed
CPC -	Condensation Particle Counter
DFB -	Dual Fluidized Bed
DMA -	Differential Mobility Analyzer
EDS -	Energy Dispersive Spectroscopy
ELIF -	Excimer Laser Induced Fluorescence
FID -	Flame Ionization Detector
FR -	Field Reversal
FR-SID -	Field Reversal Surface Ionization Detector
GC -	Gas Chromatography
ICP-OES -	Inductively Coupled Plasma Optical Emission Spectroscopy
IP -	Ionization Potential
MS -	Mass Spectrometry
MBMS -	Molecular Beam Mass Spectrometry
PIXE -	Particle Induced X-ray Emission
SI -	Surface Ionization
SID -	Surface Ionization detector
SMPS -	Scanning Mobility Particle Sizer
SPA -	Solid Phase Adsorption
TDLAS -	Tunable Diode Laser Spectroscopy
UV-VIS -	Ultraviolet Visible Spectroscopy
VTDMA -	Volatility Tandem Differential Analyzer
XRD -	X-ray Diffraction
XRF -	X-ray Fluorescence



*Once you stop learning, you start dying*

-Albert Einstein



# 1. Introduction

Increased CO<sub>2</sub> emission has led to alarmingly high concentrations of greenhouse gases in the atmosphere. The impact on the global climate may be severe and increased temperatures may pose a threat to important ecosystems.<sup>1</sup> To mitigate climate change, we need to take actions that limit the consumption of fossil resources. Biomass, which is considered CO<sub>2</sub>-neutral, can serve as a substitute to several of the fossil products we depend on today. Biomass is a multipurpose feedstock, and can be used to produce fuels, materials, and chemicals, often with minimal changes to application and distribution infrastructure.<sup>2</sup> In addition to environmental concerns, improved utilization of biomass can be important for future energy security.

At present biomass makes up around 10% of the world's total energy consumption, and is primarily used by inefficient means.<sup>3</sup> By applying a more advanced conversion process, higher efficiencies and more sophisticated products can be produced. Gasification is considered as one of the key technologies in the advancement of biomass conversion.<sup>4</sup> By applying a high temperature the biomass is decomposed into a product gas consisting mainly of H<sub>2</sub>, CO, CO<sub>2</sub>, CH<sub>4</sub>, depending on the gasification technology. However, the product gas also contains condensable materials, which can be problematic during cooling and upgrading of the gas.

Tar and alkali metals are two types of condensable components present in the product gas, which both have significant impact on the process and are the main focus of this thesis. Tar consists of a wide range of organic compounds that forms during gasification. Tar compounds are undesirable because they readily condense as the temperature is reduced, which may result in clogging and fouling of downstream equipment. Tar formation also constitutes a loss, as carbon and hydrogen instead could have been converted to desired products. Tar formation is considered as one of the main barriers for large-scale commercialization of biomass gasification. Alkali metals can also be released during gasification, and are known to form deposits with consequent agglomeration and corrosion of process equipment such as catalysts, coolers, and filters. Besides, alkali metals may have some advantageous catalytic features, which could improve the carbon conversion.

Even though there have been several studies on tar and alkali interactions during conditions relevant to biomass gasification, the mechanistic details remain unclear. One of the limitations

for gasification development has been the absence of reliable and accessible analytic tools for alkali metals and tar with sufficient time and data resolution. Thorough characterization of the product gas requires expensive and sophisticated equipment, and studies under industrial-scale conditions are scarce.

Furthermore, the harsh environment of the gasifier makes such measurements cumbersome. Both extractive and *in-situ* measurements have some inherent challenges, mainly owing to the high tar and particle concentrations. As a consequence, there is still a knowledge gap on tar formation, tar reforming, and tar interactions with inorganic compounds.

The aim of this work is to develop and apply new measurement methods, in order to improve the current understanding of the thermochemical conversion of biomass. Online measurement techniques with sufficient time resolution have been developed and applied to industrial-scale facilities. With improved chemical understanding of the process, new advanced facilities can be constructed and ultimately the next generation bio-refineries will potentially outperform today's fossil-based industry.

## 2. Background

### 2.1 Utilizing biomass

Biomass is a valuable source of energy, generated by plant photosynthesis. It provides a potentially CO<sub>2</sub>-neutral feedstock that could substitute several of the fossil products we are depending on today and can serve as an adjustable energy source in a renewable energy mix consisting of wind, solar, and biomass.

Today biomass is mainly used for energy purposes, and one third of the world's population still relies on biomass for household cooking.<sup>3</sup> With increased population growth and energy consumption, biomass demand is expected to grow. National action plans to meet national and international climate targets frequently suggest increased utilization of biomass. In Europe, biomass is expected to be a cornerstone of the renewable energy system, accounting for more than 50% of the renewable energy production by 2020.<sup>5</sup> In addition, the EU countries are mandated to incorporate 10% renewable fuels in the transport sector and 20% renewable resources in the energy sector by 2020.<sup>5</sup> Consequently, a further development of the biomass utilization and conversion is required to meet increased demands.

It is also important to consider the environmental impacts. Assessments of biomass consumption on a sustainable basis, including impact on bio-diversity and local communities, are not fully developed and long-term governmental regulations and frameworks are lacking.<sup>6</sup> Besides, emissions from biofuel combustion includes high levels of aerosol particles<sup>7</sup>, which could have severe health and climate effects.<sup>1, 8</sup> Nevertheless, it is evident that improved methods to convert biomass into valuable products such as fuels, chemicals and materials, are required in the future.

### 2.2 Biomass gasification

Having defined the important role of the biomass feedstock, let us now consider one of the techniques available for thermochemical biomass conversion – gasification. Gasification of

biomass is performed by partial oxidation of the carbon compounds at high temperatures, using air, CO<sub>2</sub> or steam. The composition of the produced gas depends on operational parameters, biomass composition and gasification technology. Several gasification technologies exist, and the end use determines which technology that is most suitable.

For example, dual fluidized bed (DFB) gasification is a technique capable of generating a product gas suitable for high-end products.<sup>9</sup> In DFB gasification, two reactors are connected by a circulating bed. By using steam as the gasification medium, a product gas with a heating value of 10-18 MJ m<sup>-3</sup> is generated.<sup>4</sup> Energy for the endothermic gasification reactions is provided from the exothermic reactions in the combustor, via the circulating bed material.

DFB gasification has gained increased attention due to its ability to use low-cost biomass feedstock. In addition, the method allows process-integration with refineries or heat and power facilities. Furthermore, power-to-gas applications can readily be employed to improve the process efficiency, with potential energy storage applications.<sup>10</sup>

In addition, advanced biomass gasification technology, such as DFB, allows flexible production streams from a versatile feedstock. After the biomass constituents are converted to gas, it can be upgraded to basically any molecule of interest. However, a high-purity gas is required in order to be able to upgrade the product gas to advanced products. Hence, effective removal of impurities is a key issue for the commercial implementation of gasification.<sup>11</sup> Gas cleaning methods are divided into primary measures related to treatments inside the gasifier and secondary methods involving gas cleaning downstream of the gasifier. Removal of impurities in the hot gas stream is costly and not always sufficient, why primary tar reduction methods including the use of additives and active bed materials receive increased attention.

Recent development has focused on catalytic tar reduction by using active bed materials, like olivine, dolomite, and ilmenite.<sup>12-15</sup> The bed material interacts with inorganic elements from the biomass, forming a surface layer that can promote tar conversion. The formation of the active ash layer and the catalytic effect is confirmed in several studies.<sup>16-18</sup> However, there is still a knowledge gap on how the ash layer is affected by the multiple redox shifts it experiences from the circulation between the two reactors. Alkali metal compounds is one of the key ash elements in this process, due to its mobility and reactivity.

In summary, biomass gasification is a powerful technology, which has a large potential in the transition towards a more sustainable society. However, impurities such as tar and alkali metals remain a technical challenge, and improved measurement methods would be valuable for the further development of the process.

## 2.3 Tar measurements

### 2.3.1 Classification of tar

Tar is classified in different ways depending on the applied measurement methods and end use of the product gas. One classification that allows concise presentation and provide adequate molecular detail for several applications was given by van Paasen et al. and is presented in Table 1.<sup>19</sup> The individual tar compounds are grouped into five classes based on their behavior in downstream processes. This classification is useful for the purpose of this thesis, since the method developed in this work observe compounds corresponding to  $\geq 4$ -ring polyaromatic hydrocarbons (class 1 and 5). However, additional classifications are also available in the literature. For kinetic modelling and mechanistic research, more detailed molecular information may be required, whereas for industrial use a total gravimetric tar analysis may be sufficient.

**Table 1.** Tar classification based on physical properties, water solubility and condensation.

	Description
<b>Class 1</b>	GC-undetectable tars. Includes the heaviest tars that readily condense at high temperatures.
<b>Class 2</b>	Heterocyclic components. Typically compounds with high water solubility, due to polarity.
<b>Class 3</b>	Aromatic compounds. Lighter hydrocarbons that do not readily condense.
<b>Class 4</b>	Light polyaromatic hydrocarbons (2–3 ring compounds).
<b>Class 5</b>	Heavy polyaromatic hydrocarbons (4-7 ring compounds).

### 2.3.2 Tar measurement techniques

As stated above, tar measurements are problematic due to the complexity of the tar compounds and the extreme conditions in the gas stream. The high variety of different processes and different types of end use makes it difficult to develop a generic measurement method. In addition, the calibration procedure can be difficult and is conventionally performed on a mixture of a few tar.<sup>20</sup>

An overview of the reported tar measurement techniques is presented in Table 2. In general, tar measurements can be divided into online and offline techniques. Offline methods are based on adsorption of the hot tar vapors, either in solvents or in dry capillaries. A sample stream of hot raw gas is extracted and passed through the adsorption medium. The samples are thereafter stored and transported to the analyzer. Offline methods are considered reliable and are widely used in industrial applications.<sup>21-23</sup> However, offline methods are not always sufficient, especially during research and commissioning, and sampling and analysis procedure may be time-consuming.

**Table 2.** Reported tar measurement methods.

Method	Sampling	Analysis
<i>offline</i>		
Tar Protocol	<i>Adsorber</i> Liquid solvent	GC-FID/MS
Peterson column	Liquid solvent	GC-FID/MS
Solid Phase Adsorption	Amine	GC-FID/MS
Carbon Nano Tubes	Active carbon	GC-FID/MS
-----		
<i>online</i>		
Laser induced fluorescence	<i>In situ</i>	Optical
Raman spectroscopy	<i>In situ</i>	Optical
Photo ionization detection	<i>In situ</i>	Optical
Molecular Beam Mass spectrometry	Extraction	MS
Ion Molecule Reaction Mass Spectrometry	Extraction	MS
Volatility Tandem Mobility Analyzer	Extraction	Thermal
Online Tar Analyzer	Extraction	FID
Liquid Quench	Extraction	UV-vis

Reported online methods either require optical access for in-situ measurements, or relies on continuous gas extraction to an analyzer.<sup>24-32</sup> In situ measurements provide a unique data set, which can be both spatially and time resolved. However, contamination of the measurement window and the high optical density in the raw gas remain as technical barriers. Additional techniques for estimating tar levels include thermal analysis to obtain the elemental yields<sup>33</sup>, and combinations of the described methods.

Extractive online measurements rely on robust gas extraction and conditioning. The sample gas is either directed to the analyzer or quenched and subsequently transferred to the analyzer. Available analyzers range from simple optical setups to complex multi-component sensors. For example, mass spectrometry methods generate detailed molecular compositional data with high time resolution.<sup>27,29</sup> However, capital and operational costs are often high, and the data analysis may require skilled personal. Continuous measurement techniques with relatively long sampling time are conventionally classified as semi-online methods, and include the tar analysis method developed within this thesis.

## **2.4 Alkali metal measurements**

### **2.4.1 Alkali metal release during gasification**

We next turn to the alkali metals, and briefly review their release behavior during gasification and relevant measurement methods. K and Na are essential elements for all living plants and therefore present in all forms of biomass. The uptake and distribution are influenced by growth conditions, plant properties and other agricultural factors.<sup>34</sup> Alkali metals exist both within the organic structure and the inorganic matrix.<sup>35</sup> As a consequence, alkali metals volatilize at two different temperature intervals during thermochemical conversion; primary pyrolysis (<500 °C) and char burnout (>500 °C).<sup>36</sup> Volatilization at low temperatures is less pronounced and corresponds to the organically associated alkali metals. The alkali metals are released as hydroxides or as part of volatile organic molecules.<sup>37</sup> In contrast, most of the alkali metal release occurs at the higher temperature interval and is associated with chlorides, carbonates and char-bound alkali metals.<sup>37</sup>

The biomass composition has a pronounced effect on alkali metal release.<sup>38</sup> For example, the availability of chlorine has a significant effect of alkali metal volatilization, due to the formation of alkali chlorides that readily evaporate. Other elements that form alkali metal compounds include silicates, carbonates, and sulfates. In conditions relevant for DFB techniques, the properties and composition of the bed material is one of the key factors influencing the alkali metal behavior. Alkali metal interactions with the bed material is discussed in further detail in section 2.5.

In summary, alkali metals play an important role in thermochemical biomass conversion and reliable and adequate measurement methods are needed to understand and control their release patterns.

#### **2.4.2 Alkali measurements in biomass gasification**

A summary of reported alkali measurement methods applied in biomass gasification is presented in Table 3. Offline techniques depend on particle collection and subsequent analysis and may provide details on alkali composition, although with limited time resolution. The development of an online technique is the subject of this work, and therefore the emphasis is on the online methods.

Despite the important role of alkali in gasification processes, online monitoring of alkali concentrations is relatively scarce. As mentioned above, the challenging conditions due to high particle and gas concentrations make both extractive and in-situ measurements cumbersome. Laser-based methods including excimer laser induced fragmentation fluorescence (ELIF)<sup>25</sup> and tunable diode laser absorption spectroscopy (TDLAS)<sup>39</sup> have been applied to determine concentrations *in situ*. In ELIF measurements UV light was used to photo-fragment alkali chloride and hydroxide molecules, and the fluorescence from excited atoms formed in the process was used to determine total alkali concentrations.<sup>25</sup> Using this method concentrations in the ranges 140 - 350 and 1.7 - 60 ppb were determined for potassium and sodium, respectively, during biomass gasification in a bubbling fluidized bed (BFB) reactor. In situ TDLAS measurements were applied to follow changes in K(g) concentration in an air-blown 100 kW<sub>th</sub> entrained flow biomass gasifier and concentrations up to approximately 1 ppm were measured depending on conditions.<sup>39</sup>

Other on-line methods rely on continuous extraction of product gas. One recent study used product gas sampling followed by inductively coupled plasma optical emission spectroscopy (ICP-OES) to study sodium release during biological waste gasification and pyrolysis.<sup>40</sup> Molecular beam mass spectrometry (MBMS) has also been applied to detect K and Na compounds in fluidized bed gasification of different biomass fuels.<sup>41</sup> Other extractive methods include the volatility tandem mobility analyzer (VTDMA) and surface ionization (SI) method developed within this work.

A few studies using SI techniques for on-line alkali detection have been reported. Olsson et al.<sup>42</sup> used the method for pressurized fluidized bed gasification and for characterization of alkali emission from associated filter ash and fluidized bed samples. Kowalski et al.<sup>43</sup> used a similar SI instrument and detected alkali species released from single grass pellets in a small laboratory-scale gasifier. Wellinger et al. used an alternative SI setup to increase the total area of the hot filament where ionization of alkali occurs and to reduce problems with turbulent flows and deposits caused by tars and particles,<sup>44</sup> and the instrument was successfully applied in time-resolved measurements in a laboratory-scale BFB gasifier fed with wood pellets.

In general, the majority of earlier studies concern alkali concentrations in laboratory-scale gasifiers and limited information is available concerning the conditions in industrial-scale processes.

**Table 3.** Reported alkali metal measurement methods.

<b>Method</b>	<b>Procedure</b>	<b>Analysis</b>
<i>offline</i>		
Particle collection	Cyclone/Filter	EDS, PIXE, XRD, XRF
<i>online</i>		
Excimer Laser Induced Fragmentation Fluorescence	<i>In situ</i>	Optical
Tunable Diode Laser Absorption spectroscopy	<i>In situ</i>	Optical
Surface Ionization	Extraction	SI
Inductively Coupled Plasma Optical Emission Spectroscopy	Extraction	Optical
Volatility Tandem Mobility Analyzer	Extraction	Thermal

## 2.5 Alkali metals in DFB gasification

So far this thesis has discussed the importance of the condensable impurities in the product gas and how they can be measured. This final section of the background will address some of the important attributes of the alkali metals, including their catalytic effect on the thermal conversion of biomass, while only a limited discussion about other important elements such as Ca, Fe and Mg is included. Another significant effect of alkali metals is their corrosive nature, which can cause severe damage on any type of biomass thermochemical conversion facility.<sup>45-46</sup>

As mentioned previously, the thermal decomposition of biomass is influenced by the presence of inorganic elements. Earlier research clearly show that the distribution and yield from thermally treated biomass is shifted towards higher gas yields and decreased condensable organics in the presence of alkali metal and alkaline earth metal compounds.<sup>47</sup> Previous studies suggest that the presence of alkali metal compounds favors the formation of low molecular weight hydrocarbons by inhibiting glycosidic bond cleavage.<sup>48</sup> Different models have been proposed to explain the mechanistic routes of cellulose pyrolysis, with some inconsistency regarding decreased formation of the tar precursor levoglucosan, or enhanced reforming of levoglucosan.<sup>49-51</sup> Patwardhan et al.<sup>48</sup> have found that glucoaldehyde and other light compounds are produced directly from cellulose, without intermediate levoglucosan formation. The authors conclude that the primary pyrolysis step consists of competing decomposition routes, and that the presence of alkali metals are active in the initial cleavage of the cellulose structure.<sup>52</sup> In addition, it has been proposed that alkali metal ions can induce hemolytic scission of various bonds in the pyranose ring.<sup>53</sup> That would generate light carbon compounds (e.g. CO, CO<sub>2</sub>) directly from the cellulose polymer. Besides, alkali metals have an effect on tar reforming, and several studies report a catalytic effect using various types of alkali metal salts.<sup>54</sup>

Another important aspect is the interaction between the alkali metals and the bed material, which is one of the key influencing factors for the type of alkali metals present and their vapor pressure. In a DFB system, where the bed material is repeatedly shifted between oxidizing and reducing conditions as illustrated in Figure 1, the alkali metal flux is complex. Observations of high K:Ca ratios for fresh bed material suggest that the initial ash layer formation is likely due

to bed material reactions with gaseous alkali metal species.<sup>16, 18</sup> Subsequently, the ash layer reacts with Ca, forming more stable Ca-silicates and the alkali metal vapor pressure is thus increased. Catalytic effects have been observed for the Ca-rich ash layer in both olivine and quartz studies.<sup>55</sup>

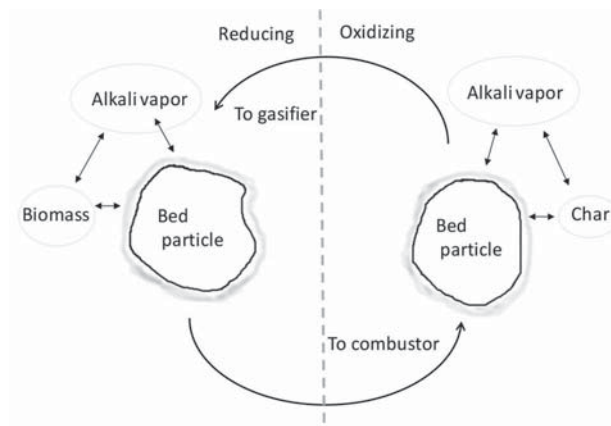


**Figure 1.** Illustration of alkali metal interactions with the bed material in a DFB gasifier.

In conclusion, the catalytic effect of alkali metals is an important tool that may be used to modify the biomass conversion process. However, it is not clear from the literature whether the effect is most important in the primary (inhibition of tar formation) or secondary step (tar reforming). In addition, care should be taken when extrapolating laboratory findings to more complex industrial environments.

## 3. Experimental techniques

In the following chapter, the experimental methods are described, from conceptual ideas to applications. The measurement techniques are adapted from aerosol science, and modified to suit the harsh environments encountered in thermochemical conversion. Novel techniques based on SI have been further developed to increase simplicity and economic viability.

Conducting measurements on a complex gas mixture at 800 °C is challenging. Either we need analyzers that can sustain the high temperature, or we need to cool the sampled gas. Since few diagnostic tools are capable of such a high temperature, the sample gas is typically cooled. Consequently, it is inevitable that a fraction of the condensable components will condense, creating biased results and measurement artefacts. This thesis attempt to turn problems associated with condensation around, and used it as an advantage. By enhancing nucleation and condensation in a controlled procedure, the condensable components will be prone to appear in the particle phase where they can be observed by aerosol analysis techniques.

### 3.1 Controlled nucleation

As explained above, throughout the field work the measurement strategy was similar: to quickly quench and cool the sample gas in order to generate aerosol particles. The nucleation is controlled by step-wise dilution of the sample gas, using a series of diluters. The setup was altered and different dilution trains were used depending on the situation at hand. Several combinations of diluters were tested during laboratory experiments prior to the field campaigns. New diluters were designed and evaluated to improve the robustness and match the specific site requirements. Designing a continuous gas extraction system for harsh environments needs careful consideration. Inadequate cooling of the sample gas may cause fouling or blockage, which will lead to signal decay and increased uncertainty.

Regarding dilution, a porous cylinder diluter was used as a first dilution step. The dilution ratio of a porous cylinder can be altered by changing the flow of dilution gas through the porous media. The length of the porous media and the flow rates are critical to prevent condensation of sample gas components on the wall. The applied cylinder diluter is depicted

in Figure 2. It consists of a perforated steel tube that is enfolded by several layers of fine mesh. The dilution flow was controlled by a mass flow controller, and a typical dilution factor for the porous cylinder was between 5 and 10.

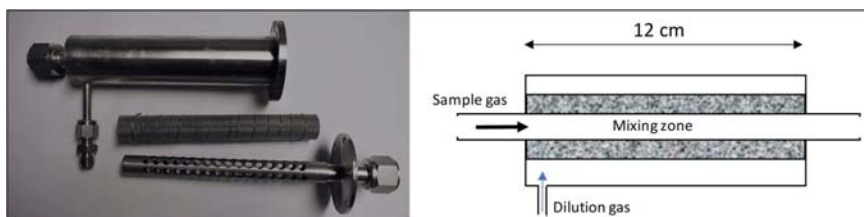


**Figure 2.** Photograph (dismantled) and schematic of the porous cylinder diluter.

During most of the experiments, ejector diluters were used downstream of the porous cylinder diluter. The ejector diluters provide a positive pressure downstream of the dilution point, caused by the large gas flow around the ejector nozzle.<sup>56</sup> This is valuable when distributing the sample gas to several instruments with different pumps, which may otherwise struggle to achieve sufficient sample gas flow. On the other hand, ejector diluters often consume high volumes of dilution gas, which could be problematic to supply and dispose of. Furthermore, the suction created by the ejector depends on the pressure in the sampling line, and it is not possible to tune the dilution factor. A photograph of three ejector diluters connected in series is presented in Figure 3.

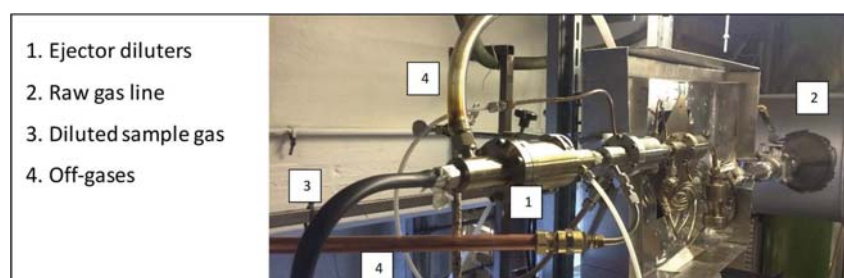


**Figure 3.** Three ejector diluters mounted in series and connected to the product gas line at the Chalmers gasifier.

The simultaneous rapid changes in temperature and dilution ratio make the condensation process complex, and volatile compounds with a saturation pressure above a certain level will not condense.<sup>57-58</sup> Regarding alkali metals, gas-phase constituents can be neglected, owing to

the low saturation vapor pressure at the temperature when the sample gas passes the analyzer (25 °C). In contrast, several tar compounds are volatile and their vapor pressures may be significant, in particular for the lighter tar compounds. Thus, the degree of condensation for pure tar compounds was estimated from a kinetic model described in section 3.3.1. The model describes the evaporation of a single aerosol particle, and selected evaporation profiles are illustrated in Figure 4. As a first-order approximation, compounds that completely evaporate below 25 °C were considered not detectable, whereas other compounds were reported as “heavy tar”. This estimation would seem to suggest that the threshold for condensation appears between class 4 (light polycyclic aromatics) and class 5 tar (heavy polycyclic aromatics).

In addition to the kinetic model, aerosol partitioning theory<sup>59</sup>, which describes the partitioning between solid/liquid and gas-phase was used to validate the estimated condensation patterns.<sup>59</sup> Partitioning calculations require knowledge of the gas composition, along with the particle loading and physical properties of the gas. A typical particle-to-gas partitioning is given in Figure 4. The estimated extent of condensation is comparable to that obtained from the kinetic model, and a condensation threshold appears between anthracene and fluoranthene.

The condensation estimates have to be approached with some caution, because of several influencing parameters. Nevertheless, condensation profiles for tar and alkali metals are valuable for any process that includes product gas cooling.

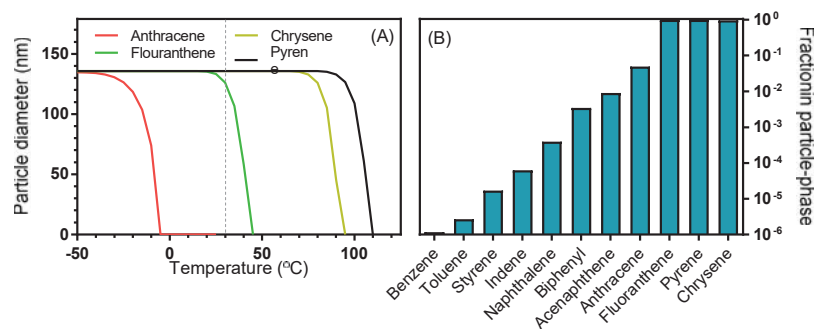


**Figure 4.** A: Calculated evaporation profiles for selected tar compounds. The dashed line indicate the temperature in the particle analyzer, thus compounds to the left side of the line will not be detected as particles in the sample gas characterization. B: Calculated degree of condensation for selected tar compounds, based on aerosol partitioning theory.

Let us now consider how the condensable components can be characterized and how the particle size distribution is used for composition analysis. The aerosol particles in the sample gas exhibit a wide range of particle diameters, and a simplified illustration of the different modes is given in Figure 5. By applying a combination of aerosol measurement techniques, the size distribution of particles can be characterized and evaluated. During the field measurements, up to three modes were identified, which could be associated with the different components in the product gas. As indicated in Figure 5, condensed gas components will mainly end up in the nucleation mode, due to the available surface area, while most primary particles will be larger. The particle composition was further analyzed, using thermal stability analysis, either by heating the entire particle distribution, or by selecting a narrow size interval. The aerosol particles are directed to a high temperature oven and the evaporation is observed. The oven temperature can be either fixed, or in scanning mode, and the thermal analysis is described in further detail below.

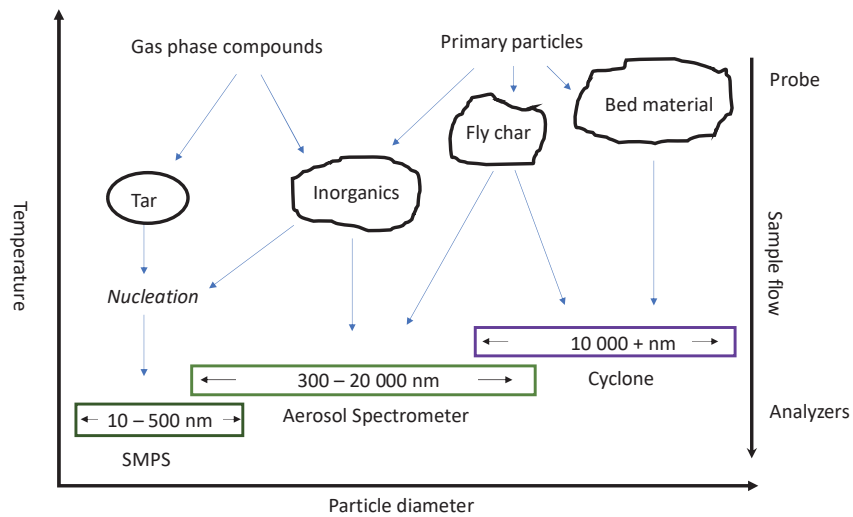


**Figure 5.** A simplified illustration of the nucleation and particle distribution, including typical measurement ranges for the different aerosol measurement techniques applied.

## 3.2 Aerosol characterization techniques

### 3.2.1 Scanning Mobility Particle Sizer (SMPS)

In several experimental setups reported in this work, a scanning mobility particle sizer (SMPS) was used to characterize the aerosol size number distribution. The concept was introduced during the 1970's and has been used extensively for aerosol particle studies.<sup>60</sup> The system consists of a differential mobility analyzer (DMA) and a condensation particle counter (CPC). The DMA classifies aerosol particles according to their electrical mobility, and the principle is illustrated in Figure 6. By applying a negative voltage along a vertical sample flow, positively charged particles will be attracted and start to migrate towards the opposite side of the electrical field. For a given field strength, particles with a certain electrical mobility ( $Z_p$ ) will migrate towards the opposite charge, and pass through an exit slit. Uncharged particles and particles with different mobility will follow the excess flow stream and are filtered out. If the

particles are charged by bipolar diffusion, a Boltzman equilibrium charge distribution is obtained, and the particle size can be associated with a specific voltage according to:<sup>61</sup>

$$Z_p = \frac{n e C}{3 \pi \mu d_p} \quad (1)$$

where  $n$  is the number of charges,  $e$  is the elementary charge,  $C$  is the Cunningham slip correction,  $\mu$  is gas viscosity, and  $d_p$  is the particle diameter.

Downstream of the DMA, the particles are counted by the CPC. Here, the particles grow into droplets that can easily be counted using an optical detector in two steps; First, the particles enter a chamber with saturated vapor, e.g. butanol or water. Thereafter the sample gas is cooled to create super saturation whereby the vapor will condense on the aerosol particles, which will grow into droplets that are detected by light scattering. By scanning the DMA voltage exponentially, the measurement time for the entire size range can be reduced. The SMPS time resolution is a trade-off between size and time resolution, and was typically between 60 - 300 s, allowing a measurement size range of 10-500 nm. To obtain a particle number size distribution, the data stream from the CPC is processed with a data inversion which accounts for DMA voltage, charge distribution, CPC efficiency, DMA transfer function, diffusion losses, and properties of the sample gas.

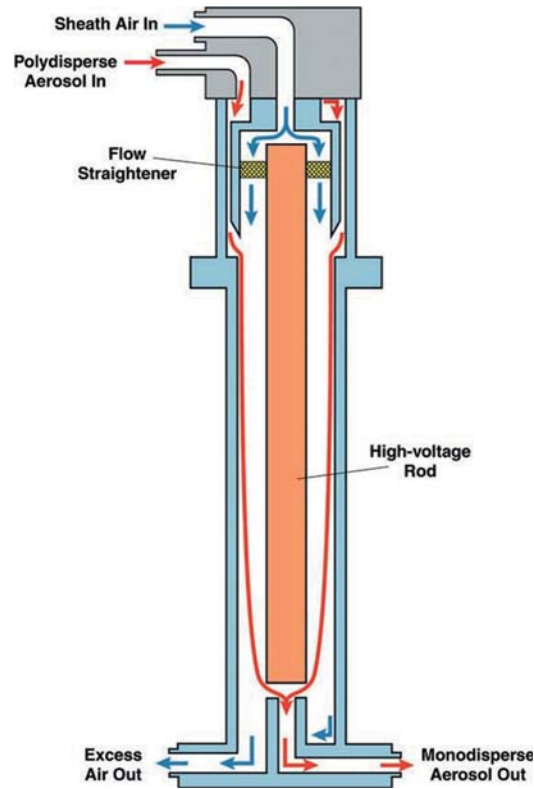


Figure 6. Schematic illustration of the DMA (Illustration from TSI Inc.)

### 3.2.2 Optical aerosol spectrometer

Optical aerosol spectrometers have the advantage of being small and portable units that enables continuous measurements of particle number and mass concentrations with high time resolution. The particles pass through a light source and the scattered signal is transferred to a recipient diode. The spectrometer used in this thesis is the Spectrometer 1.108, manufactured by Grimm Aerosol Technik Ainring GmbH & Co. It operates with a laser that alternately scans particles for 3 s at 0.5 mW to detect large particles, and another 3 s at 30 mW to detect small particles.<sup>62</sup> The number concentration is simply obtained by counting the number of pulses, and the corresponding particle size is determined from the magnitude of the pulse.<sup>63</sup>

### 3.3 Thermal stability analysis

The thermal properties of the aerosol particles were investigated using a high temperature oven. A coiled gas line passes through the oven, with a total length of 2.02 m, which provide a residence time of a few seconds. The oven can be heated to 1000 °C and is illustrated in Figure 7. As discussed in section 3.1, the obtained particle size distribution from the controlled nucleation can be represented by a linear fit of up to three log-normal distributions (modes). Figure 8a. shows a particle size distribution from biomass gasification product gas, and the linear combination of three lognormal distributions. When the aerosol particles are heated to 400 °C, the nucleation mode (mode 1) formed by condensed tar evaporates. This is illustrated in Figure 8b, where the product gas passes through the oven. The evaporated mass fraction is used to determine the mass concentration of heavy tars present in the sample gas.

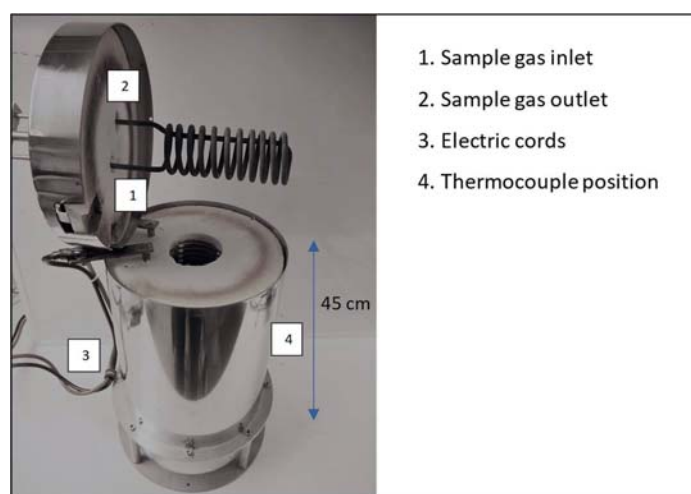
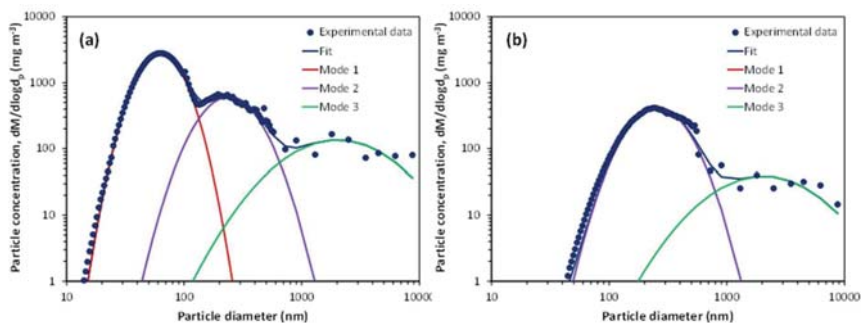


Figure 7. A photograph showing the high temperature oven (dismantled).



**Figure 8.** Particle mass size distributions, a) normal sampling; b) after the sampled aerosol has passed through a 400 °C oven before reaching the instruments. The figure include least square fits of the data (dark blue line) using a linear combination of three lognormal distributions. The individual lognormal distributions are marked Mode 1-3 (red, purple and green lines).

For kinetic calculations, the temperature profile within the heated zone is considered homogenous and a plug-flow model was used to calculate particle volatility. The temperature is measured with a thermocouple inserted in the center of the oven. Different compounds will evaporate within narrow temperature intervals. The obtained evaporation profiles can be used to chemically characterize the sampled aerosol particles, in a similar way as the thermogravimetric analysis (TGA)<sup>64</sup> for solid samples. By continuously extracting a gas flow, the method can be used for online measurement, where heating rate and response time of the analyzer limit the sampling rate. The evaporated particle mass can be calculated from the number concentration, assuming spherical particles and a homogenous density.

### 3.3.1 Volatility Tandem DMA (VTDMA)

A more sophisticated thermal analysis can be performed by examination of a monodisperse aerosol. By using an additional DMA, size-selected particles can be extracted from the sample gas and subsequently analyzed using the oven and the SMPS system. The principle is illustrated in Figure 9.

The VTDMA method has previously been used in aerosol research to characterize combustion aerosols and to investigate thermal properties of secondary organic aerosols.<sup>65-70</sup> The method is based on the principle that different condensed components evaporate in characteristic temperature ranges. By increasing the temperature of the oven while continuously observing the particle diameter, the reduction in particle size can be linked to chemical constituents. The VTDMA system is illustrated in Figure 9, together with the particle generation setup used to evaluate the performance of the instrument in the laboratory.

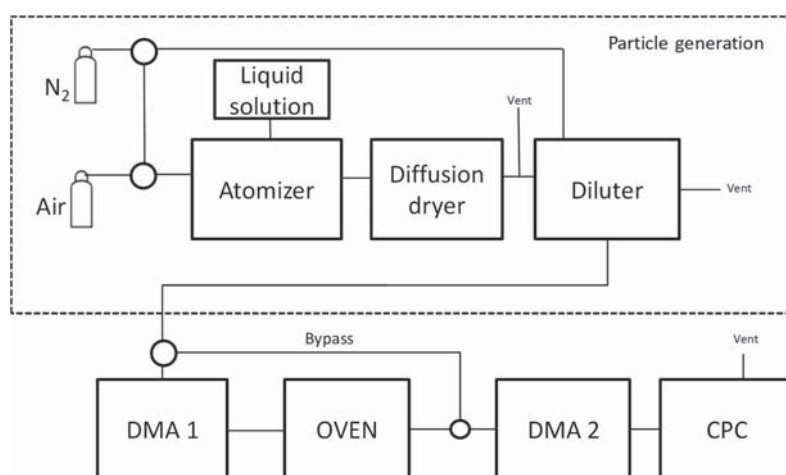
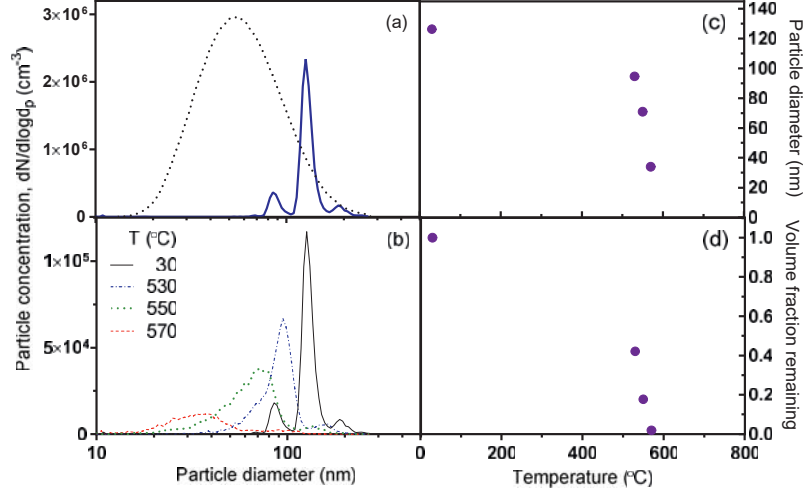


Figure 9. VTDMA setup and test aerosol particle generation.

The thermal stability of the aerosol particles can be illustrated by a so called thermogram. The observed mode diameter at each temperature is converted to volume, assuming spherical particles, and the remaining volume fraction is plotted as a function of temperature. An example of KCl particles with an initial particle diameter of 120 nm, heated to different temperatures is given in Figure 10. The thermogram for pure particles can be used to identify components in a internally mixed aerosol.



**Figure 10.** Example of VTDMA analysis. A: Initial particle distribution. B: Size-selected particle distribution at different temperatures. C: The particle mode diameter as a function of temperature. D: The corresponding thermogram.

In addition, the evaporation of a single aerosol particle can be described using the following kinetic model:<sup>71-72</sup>

$$\frac{d(d_p)}{dt} = - \frac{4 D_i M_i P_i^0}{\rho_i d_p R T} \exp\left(\frac{4 \gamma_i M_i}{d_p \rho_i R T}\right) f(Kn_i, \alpha) \quad (2)$$

where  $d_p$  is the particle diameter,  $t$  is the evaporation time,  $D_i$  is the diffusivity of molecule  $i$  in the surrounding gas calculated according to Ref 72,  $M_i$  is the molar mass,  $P_i^0$  is the saturation vapor pressure,  $\rho_i$  is the particle density,  $\gamma_i$  is the surface free energy, and  $R$  is the gas constant.  $f(Kn_i, \alpha)$  is a correction term for particles in the transition regime where the particle diameter is small compared to the mean free path of the surrounding gas given by,<sup>73</sup>

$$f(Kn_i, \alpha_i) = \frac{1 + Kn_i}{1 + 0.3773 Kn_i + 1.33 Kn_i \frac{(1 + Kn_i)}{\alpha}} \quad (3)$$

where  $\alpha$  is the accommodation coefficient, which was set to unity<sup>74</sup>.  $Kn_i$  is the Knudsen number,

$$Kn_i = \frac{2\lambda_i}{d_p} \quad (4)$$

where  $\lambda_i$  is the mean free path of molecule  $i$  in the gas phase. The model takes into account the Kelvin effect that describes the increase in vapor pressure over a curved surface compared to a flat surface, while re-condensation of evaporated gas is ignored.<sup>75</sup>

### 3.4 Surface ionization technique

Surface ionization (SI) techniques has been recognized as a suitable method for alkali metal measurements.<sup>42, 76-80</sup> The SI process, whereby an atom becomes ionized upon desorption from a surface is described in Ref 82. The degree of ionization ( $\alpha$ ) for a desorbing atom is described by:

$$\alpha = \frac{n_+}{n_0} = \frac{g_+}{g_0} \exp \left[ \frac{e(\phi - IP)}{k_B T} \right] \quad (5)$$

where  $g_+/g_0$  denotes the statistical sum ratio of neutral atoms and ions, and  $e$ ,  $IP$ ,  $\phi$ ,  $k_B$  and  $T$  denote elemental charge, ionization potential, surface work function, Boltzmann's constant and surface temperature, respectively. For most elements  $IP > \phi$ , meaning that the degree of ionization is negligible. However, alkali metals are an exception with very low  $IP$ , which enable selective alkali metal measurements.

The Atmospheric Science Group at University of Gothenburg has developed several aerosol instruments based on SI technique, including Alkali Aerosol Mass Spectrometers<sup>78-79</sup> and surface ionization detector (SID) setups that operate at ambient pressure.<sup>76, 80</sup> Investigations confirm that submicron alkali salt particles give rise to ion pulses in contact with a hot platinum filament in air. The alkali atoms in individual aerosol particles are ionized by SI on the hot filament, and the emitted ions diffuse to a closely situated collector where they are detected as a current. The ionization probability may approach 100% for elements with low  $IP$ , and the method may therefore provide sensitive and selective measurements of aerosol particles containing alkali salts.

### 3.4.1 Surface ionization detector (SID)

The SID used in this work was similar to the one used by Davidsson et al.<sup>76</sup> A schematic view of the SID and a photograph of the instrument in operation are shown in Figure 11. The sample flow is passed through the measurement cell, in which a hot platinum filament is mounted. A fraction of the particles will impact on the filament and subsequently melt and dissociate. The filament is biased with a positive voltage, and part of the ions will impact on a metal plate placed in parallel to the filament. The metal plate is connected to a current amplifier, and the ionic current is proportional to the alkali metal concentration in the sample gas.

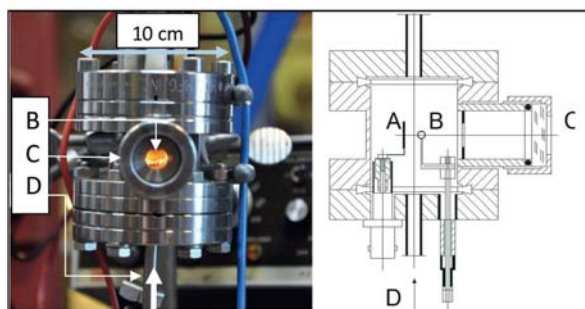


**Figure 11.** Photograph and cross section of the surface ionization detector (SID) showing A) the ion collector, B) the Pt filament, C) the quartz window and D) the sample gas flow direction.

The processes involved during the complex interaction of a submicron alkali salt particle and a platinum surface have been studied in earlier work<sup>80-81</sup>, and include particle transport to the hot surface, deposition, melting, decomposition, desorption of alkali ions, and subsequent transport of ions to a nearby collector. The work function of the surface may also be influenced depending on the sample gas composition. Furthermore, minor discrepancies in the crystal surface combined with the external electrical field, may also influence the degree of ionization (so called Schottky effect).<sup>82</sup> Nevertheless, calibration tests show a linear relation between the SID signal and alkali particle concentration in the sample gas. The SID signal corresponds to the total concentration of alkali metals in the sample gas, however, the ionization probability is slightly lower for Na compared to K. The lower detection probability for sodium salts has not been accounted for in the reported total alkali (Na + K) mass concentrations. For studies on biomass with high K:Na ratio, the deviation would provide an under estimation of the alkali mass concentration by approximately 1%.

### 3.4.2 Field Reversal – SID (FR-SID)

This section describes the further development of the SID, where a difference in desorption kinetics is used to distinguish between K and Na. The principle of the field reversal (FR) technique is to periodically block the ionic desorption from the surface by shifting the direction of the electrical field. If a retarding field is applied, the positively charged desorbing ions will be forced back towards the filament surface. For low field strengths, the desorption process itself is not significantly affected by the applied field, thus a similar SID as described previously can be used with addition of a wave generator that can switch the bias voltage at the filament surface. The basic principle of FR is illustrated in Figure 12, along with a schematic of the setup. During the retarding phase, incoming alkali metal atoms will accumulate at the surface. As the electrical field is switched to the accelerating phase, the accumulated alkali metal atoms are liberated and will desorb towards the detector. The desorption rate ( $k$ ) for different alkali metal atoms are dissimilar, and this discrepancy is used to separate the elements. The general trend is that  $k_{Na^+} < k_{K^+}$ , meaning that  $Na^+$  desorbs slower than  $K^+$  at a specific surface temperature.

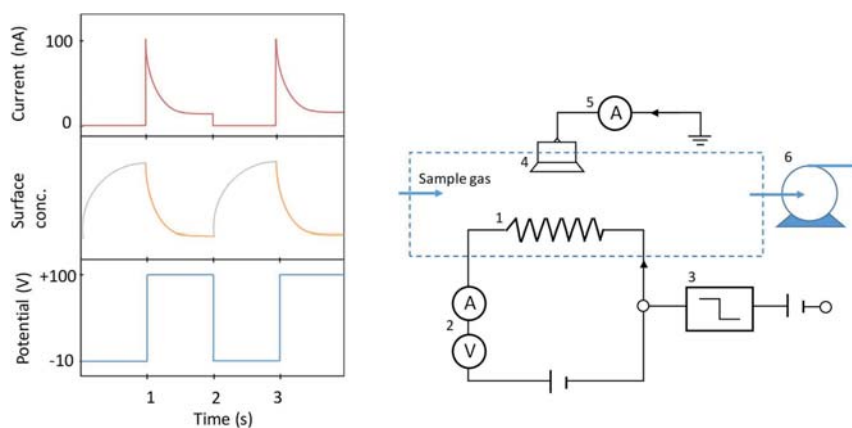


**Figure 12.** Left: Example of how the filament potential, the concentration of alkali atoms on the filament surface and the measured SID current varies with time. Right: Schematic view of the FR-SID setup. 1, Pt filament. 2, Filament current control. 3, Wave generator. 4, Collector plate. 5, Ion current monitor. 6, Sample gas pump.

### 3.5 Evaluation and calibration

The instruments were tested before and after each experiment regarding sample flow rate, temperature, zero point and leakage. Periodical calibration of the SMPS particle size classification and the SID units was performed, and are described below.

For particle size calibration, polystyrene latex spherules with diameter of 40, 100, 200 and 500 nm were used. The test aerosols were generated from a constant output atomizer. The observed particle modes were within 10% of the corresponding diameter of the spherules, and no correction on the reported data was performed. In addition, comparison measurement with a similar SMPS systems (TSI Inc, SMPS 3080) were conducted and observed particle sizes were in close agreement.

The SID calibration is based on measurements of pure KCl particles, where the SMPS system was used as reference. A linear calibration model was applied, using ordinary least square fitting, and the calibration data is presented in Figure 13, along with a histogram of the model residuals. The residuals are concluded to have a normal distribution and was used to estimate the measurement uncertainty described in section 3.5.1.

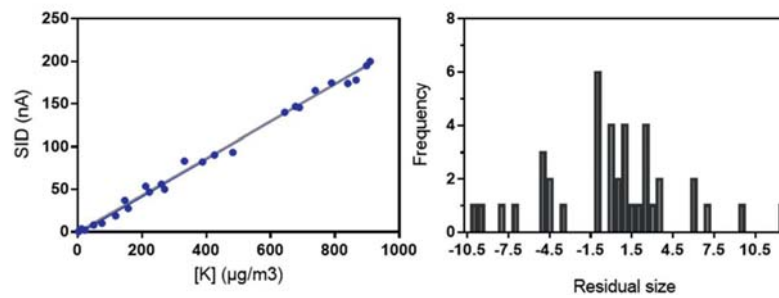


**Figure 13.** Left: Measured ion current with the SID as a function of potassium concentration in laboratory experiments with KCl particles. Right: Histogram of residuals from the least square fitting, indicating a normal distribution of the residuals.

The particle transmission through the oven was investigated using NaCl particles, which are stable over the investigated temperature interval. The NaCl particles were generated from a

constant atomizer, and the result for 100, 200 and 300 nm particles are presented in Figure 14. A linear decrease in transmission is obtained within the investigated particle size range.

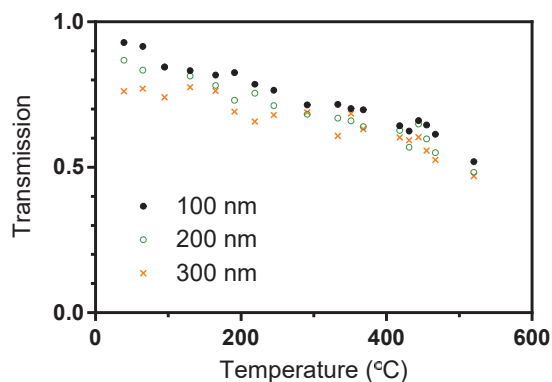


**Figure 14.** Oven transmission for NaCl particles as a function of temperature. Three different particle diameters, 100, 200 and 300 nm are illustrated.

### 3.5.1 Measurement uncertainty

In order to compare the reported values with literature data, the measurement uncertainty should be addressed. In the following, the main uncertainty components for the different instruments are discussed.

Regarding the SMPS measurements, the method has been used as a National Institute of Standards (NIST) reference for sub-micron particles for over a decade. Studies on 60 and 100 nm particles using electrical mobility classification estimate the uncertainty to be approximately 1% of the particle size.<sup>83</sup> Besides, rigorous peer-reviewed investigations have been performed and reported uncertainty in particle sizing is reported to be below 3.5%.<sup>84</sup> The CPC counting efficiency for particles with a diameter > 5 nm are close to unity, and only minor deviation occurs between different CPCs. For mass concentrations, the particle density represents the main contribution to the total uncertainty, and knowledge of the particle composition is therefore important for precise mass concentrations.<sup>85</sup>

Regarding the optical spectrometer, the reported concentration depends on the refractive index, particle shape and mixing type of the sampled aerosol.<sup>86</sup> The spectrometer is equipped

with a small filter in the exhaust line, which can be weighed and used for density corrections. The aerosol density is the main uncertainty component for optical measurements, and by applying a density correction the measurement error can be significantly reduced.<sup>86</sup>

During the field measurements the CO-ratio between the diluted and undiluted sample gas was used for estimating the dilution. The CO measurements were performed with non-dispersive infrared method and the instruments were calibrated with reference gas. Owing to the fact that the ratio of two CO observations was used, uncertainty components such as interference of CH<sub>4</sub> and CO<sub>2</sub>, are likely to cancel out. The uncertainty of the CO measurements was not assessed further, although it is worth mentioning as a possible uncertainty component.

As regards the SID measurements, the uncertainty was assessed for KCl particles using a top-down approach.<sup>87</sup> The residuals from the linear fitting were used to estimate the variance, and the relative standard deviation was 3.7%. Five uncertainty components were investigated; filament temperature, sample gas flow rate, filament voltage bias, type of alkali metal compound and particle size, were the type of alkali metal compound represents the largest uncertainty. The systematic error was not assessed.

In summary, the key uncertainty components in the measurement system was assessed and awareness of these parameters are useful for further development of the measurement system and data interpretation.

## 4. Industrial facilities

In addition to laboratory experiments, measurements were also performed at three research and industrial facilities, scaling from test-rig size to a large-scale industrial biofuel plant.

### 4.1 The Chalmers Gasifier

The Chalmers power central includes a 12 MW<sub>th</sub> combustion unit and a 2-4 MW<sub>th</sub> gasifier<sup>88</sup>, connected in a DFB setup. The system is illustrated in Figure 15. Hot bed material is transferred via a cyclone to the gasifier, delivering heat necessary for the gasification reactions. The product gas is directed to the boiler, where it is combusted for heat recovery. Measurements were performed in the main product gas channel 5 m downstream of the gasifier freeboard. The temperature in the raw gas was approximately 750 °C, which may be compared with a bed temperature between 800 and 850 °C during the experiments. Several measurement campaigns were performed at the Chalmers gasifier, with different bed materials, additives, and fluidization rates, with the aim to characterize the alkali and tar concentrations in the product gas.

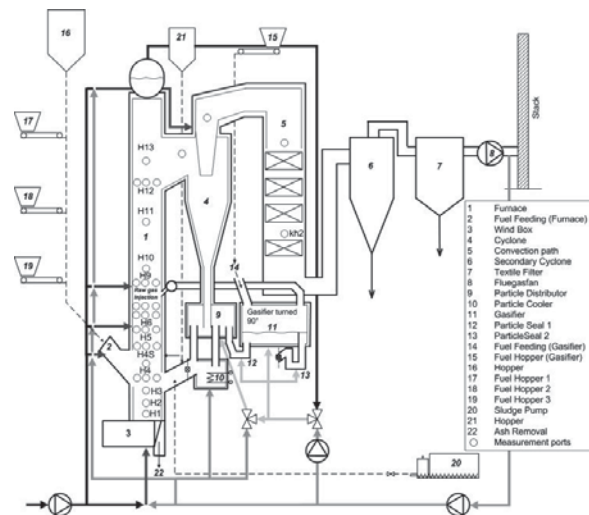
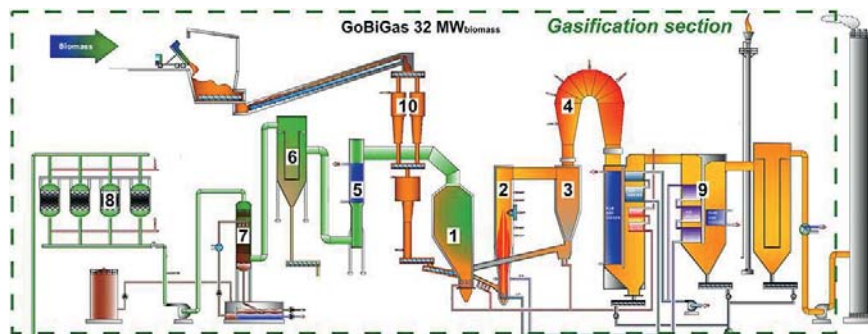


Figure 15. The Chalmers power central system.<sup>88</sup> (Illustration from Chalmers University of Technology).

## 4.2 The Gothenburg Bio-Gas facility

The Gothenburg Bio-Gas (GoBiGas) project is one of the largest DFB biomass gasification plant world wide, approximately eight times larger than the Chalmers gasifier.<sup>9</sup> It is dimensioned to produce 160 GWh of bio-methane annually, which is equivalent to the fuel consumption of 16 000 cars. The gasification section of the plant is illustrated in Figure 16. The DFB gasification unit is similar to the Chalmers gasifier and consists of a combustion reactor in which heat for the gasification is produced, and a gasifier in which the fuel is converted into gas. The fuel is primarily fed to the gasifier, which is fluidized with steam, where the fuel is devolatilized and partially gasified. Unconverted char is transported with the bed material to the combustor. Here, the char is combusted together with energy-rich off-streams from downstream processes as well as part of the product gas, which is fed back to the boiler so as to maintain and control the temperature of the process. The warm bed material is circulated back to the gasifier via a cyclone, thereby providing the heat required for the fuel conversion.



**Figure 16.** A schematic of the GoBiGas gasification section. 1, gasifier; 2, combustion chamber; 3, cyclone; 4, post-combustion chamber; 5, raw gas cooler; 6, raw gas filter; 7, rapeseed methyl ester scrubber; 8, carbon beds; 9, flue gas train; 10, fuel feeding system. (Illustration from Göteborg Energi AB).

### 4.3 Chalmers oxy-fuel test rig

Experiments were also performed in the Chalmers 100 kW<sub>th</sub> oxy-fuel test rig<sup>89</sup>, illustrated in Figure 17. The rig allows recycling of flue gases and can be operated in air- or oxygen-fired mode. It can operate with both solid and gaseous fuels. The height of the cylindrical combustion chamber is 2.4 m and the inner diameter is 0.8 m. The burner has two annular swirling air registers. Measurement ports are placed along the height of the combustion chamber to allow spatial characterization of the flame. An oil-cooled probe was used to extract sample gas from Ports M2 - M5.

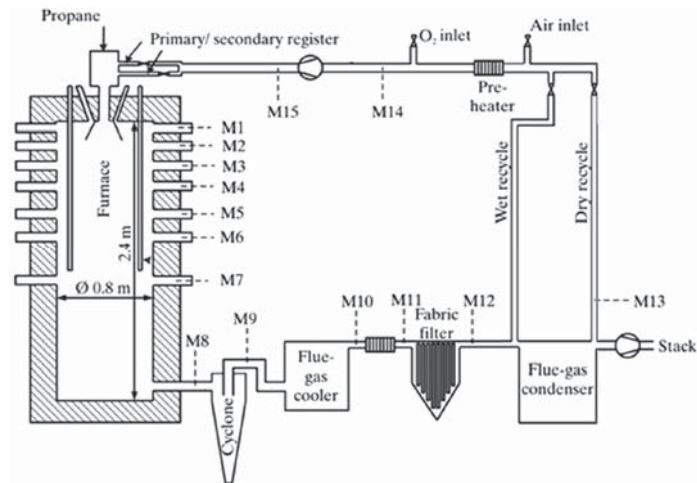


**Figure 17.** Schematic of the oxy-fuel test rig. The measurements were performed in ports M2-M5. (Illustration from Chalmers University of Technology).

## 5. Results and discussion

### 5.1 Laboratory studies

#### 5.1.1 Volatility measurements

Aerosol particles were characterized based on their thermal properties using VTDMA technique and the method was initially tested in a series of laboratory experiments (Paper I). Figure 18 shows examples of evaporation thermograms for selected potassium salts, which are expected to play an important role in biomass gasification. The particles were atomized from a liquid solution, dried and thereafter heated in the oven under inert conditions. The observed reduction in diameter reflects either molecular sublimation or decomposition and subsequent evaporation. The particle diameter of KCl decreases rapidly at temperatures above 500 °C, and the observed evaporation kinetics agree well with literature values for KCl evaporation.<sup>90</sup> The evaporation of the more thermally stable K<sub>2</sub>SO<sub>4</sub> particles takes place at substantially higher temperatures, and the evaporation is expected to be dominated by molecular sublimation and to a lesser extent by decomposition into 2K(g) + SO<sub>2</sub>(g) + O<sub>2</sub>(g).<sup>91</sup>

For the more volatile KOH, which is abundant in steam gasification<sup>92</sup>, two evaporation steps were observed. The first step corresponds to desorption of KOH, while the second evaporation step is similar to K<sub>2</sub>CO<sub>3</sub>, and is likely a carbonate residue formed from CO<sub>2</sub> contamination under the experiments. Note that compounds with a low boiling point, such as KOH, are likely to melt before evaporation is completed. The K<sub>2</sub>CO<sub>3</sub> particles undergo gradual decay at lower temperatures potentially caused by several factors, including changes in crystal structure, CO<sub>2</sub> emission, and partial decomposition of potassium bicarbonate produced during formation of the particles. Reported experiments on K<sub>2</sub>CO<sub>3</sub> volatility are limited to inert conditions, and the degree of decomposition during different gas compositions is not known. In product gas from biomass gasification, the high concentrations of CO, CO<sub>2</sub> and H<sub>2</sub>O may influence the carbonate evaporation.<sup>93</sup> In general, the high temperature carbonate – hydroxide chemistry is important

for steam gasification and the evaporation profiles can illuminate the transformation patterns during gasification conditions.

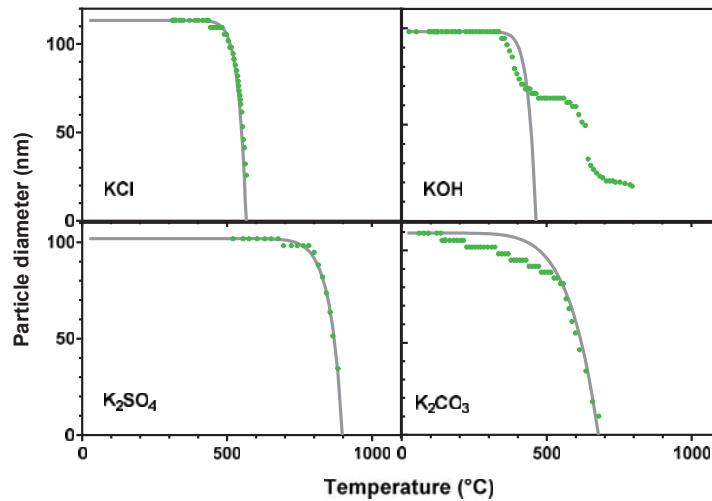


**Figure 18.** Diameter of size-selected particles as a function of oven temperature. Experimental results (points) and calculated values using a kinetic evaporation model (solid line).  $K_2SO_4$  and  $K_2CO_3$  are fitted using the saturation vapor pressure as a free parameter (eq. 2).

Another significant aspect of the VTDMA is the capability to distinguish between different compounds or group of compounds. Figure 19 illustrate the result for internally mixed aerosol particles, with KCl and  $K_2SO_4$  (1:1 molar ratio with respect to potassium). The evaporation takes place in two separate steps corresponding to initial KCl release followed by  $K_2SO_4$  evaporation in a higher temperature interval. Assuming spherical particles, the initial decrease in diameter corresponds to a reduced volume by 50%. In addition, experiments with alkali salt particles coated with tar vapor, showed that the particle core can be recovered with minimal losses. The observed step-wise evaporation indicates the potential for further development of the method.

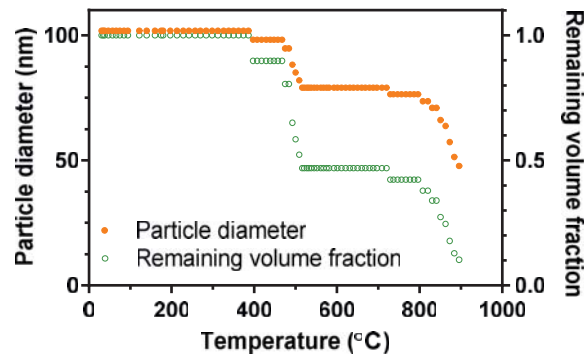


**Figure 19.** VTDMA results for mixed KCl-K<sub>2</sub>SO<sub>4</sub> as a function of oven temperature. The evaporation takes place in two separate steps corresponding to initial KCl release followed by K<sub>2</sub>SO<sub>4</sub> evaporation.

In addition to the alkali salt experiments, a limited set of laboratory experiments were carried out with organic aerosol particles. Heavy tar compounds were concluded to evaporate well below 400 °C, and are thus easily separated from the alkali metals.

In conclusion, the laboratory results suggest that VTDMA technique can be applied as a diagnostic tool for some of the important condensable components in the product gas. A main advantage with the VTDMA technique is the ability of online analysis and the possibility to simultaneously characterize condensed tar and alkali metal compounds. The VTDMA method is complementary to existing tar analysis methods based on batch sampling, such as SPA and the tar protocol (see section 2.3.2), which provide detailed information about the tar composition. In contrast, the VTDMA method provides information about the fraction of heavy tars, some of which are not easily characterized with existing laboratory techniques. In addition, the VTDMA may be used to determine the thermal stability of compounds in the temperature range of relevance to gasification processes.

### 5.1.2 FR-SID development

The Laboratory studies were also performed to evaluate the new FR-SID concept that was developed in Paper V. The setup was evaluated using aerosol particles consisting of various alkali metal salts. Measurements on KCl and NaCl particles were performed at filament

temperatures between 1230 K and 1500 K, and typical results are presented in Figure 20. The observed desorption kinetics are distinctly different for potassium and sodium salts, which can be used to distinguish them in a mixed aerosol.

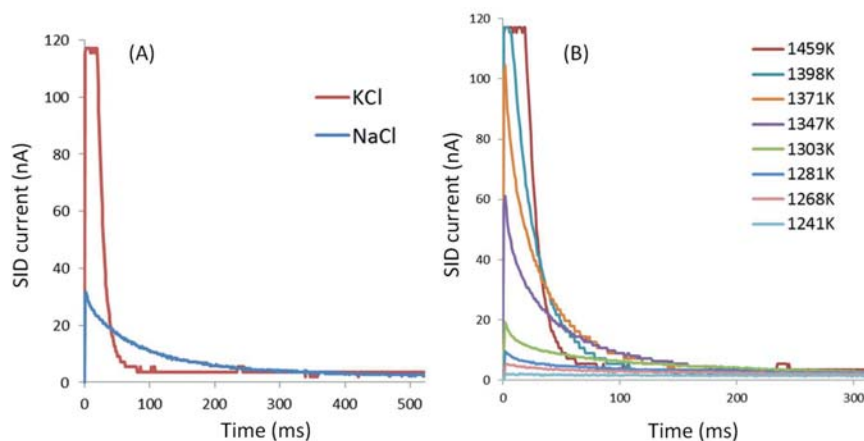


**Figure 20.** A: SID signals obtained from NaCl and KCl during the accelerating phase in a FR measurement with a filament surface temperature of 1460 K. B: SID currents obtained from FR measurement on KCl particles at eight different filament temperatures

In the aspect of applying FR technique to discriminate between K and Na, a filament temperature of 1400-1500 K was concluded to be optimal. In this range the slower Na<sup>+</sup> desorption can be observed, and the K<sup>+</sup> and Na<sup>+</sup> desorption rates are divided by at least a factor of ten. At lower temperatures, the Na<sup>+</sup> desorption became too slow to be observed on the time-scale used in the experiments.

The results from the FR-SID technique shows that it is possible to discriminate between K and Na signals obtained from SI. The concept was successfully applied in a short measurement in ambient air, and future applications are expected to include both air quality studies and alkali measurements in combustion and gasification processes.

## 5.2 Field results

### 5.2.1 Thermal stability of particles from gasification and combustion processes

The VTDMA system was applied in the three facilities described in Chapter 4 and the results are summarized in Figure 21. As can be seen from the figure, the volatility profiles are dispersed, which indicate the differences in the chemical composition of the sampled aerosols. The VTDMA system was initially tested at the Chalmers gasifier using two different sampling probes with and without thermodenuder as the major difference (Paper I). A similar measurement was also performed at GoBiGas with a different dilution system (Paper II). The GoBiGas gasifier was operating with olivine as bed material and with continuous addition of  $K_2CO_3$  to the combustor, whereas the Chalmers gasifier was operating with silica sand. Particles sampled at the Chalmers gasifier without thermodenuder consist mainly of tars (90 vol%) which evaporate at temperatures below 150 °C, while particles sampled with a thermodenuder are thermally more stable. The sampled particle distributions are illustrated in Figure 22. In addition, the particle core evaporates within a similar temperature interval, consistent with the  $K_2CO_3$  data from laboratory experiments. This is likely  $KOH(g)$  that reacts with  $CO/CO_2$  in the sampling system and forms carbonate, as discussed in the previous section. Intriguingly, the GoBiGas particles also showed a high thermal stability with three minor evaporation steps (barely visible in the figure due to the logarithmic scale). The first step is observed at 100-200 °C and is associated with heavy tars. The second step coincide with  $K_2CO_3$  evaporation, and is most likely  $KOH(g)$  from the product gas, as previously explained. For plant safety reasons the oven temperature could not be increased sufficient to evaporate the remaining stable fraction of the particles.

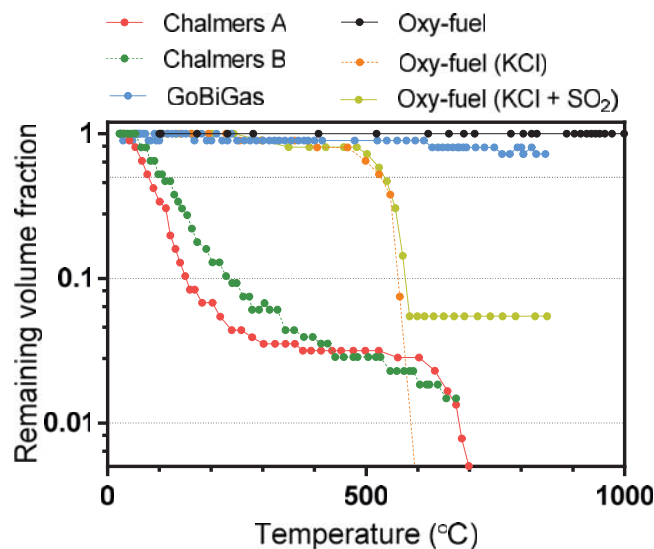


Figure 21. VTDMA results plotted as thermogram for different sample gases.

We now turn to the experiments performed at the oxy-fuel test rig (Paper IV), and results from conducted particle measurements at port 3 (see Figure 17). Particles sampled under several different flame conditions were investigated, including oxy-fuel combustion of coal particles and propane combustion with additions of KCl and SO<sub>2</sub>. The additions of KCl(aq) and KCl(aq) + SO<sub>2</sub>(g) drastically shifted the particle distribution, as seen in Figure 22.

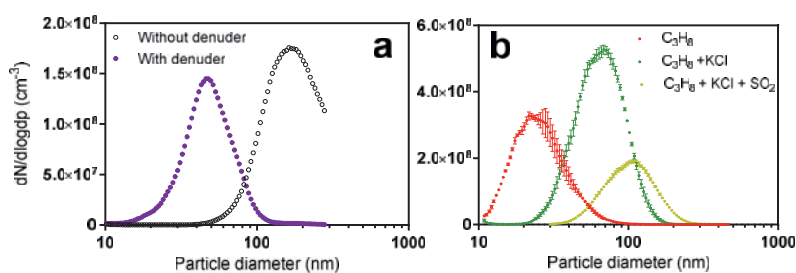


Figure 22. Particle size distribution from the Chalmers gasifier, sampled with and without thermodenuder. b: Particle size distribution from a propane flame at the Oxy-fuel test rig with additions of KCl and SO<sub>2</sub>. The error bars indicate the standard deviation.

The volatility profiles are given in Figure 21, and particles analyzed without addition corresponds to primary soot particles, which are not affected by the thermal treatment. This is in agreement with volatility studies performed by Higgins et al.<sup>94</sup>, who showed that soot particles are stable at 1100 °C during inert conditions. However, during the additions, the size selection in the first DMA was shifted towards larger particles (around 100 nm), as indicated in Figure 22. This mode was not visible prior to the additions, and stems from the added components. During KCl addition, the particles evaporate steeply within the KCl temperature range. During SO<sub>2</sub> addition, a fraction of the KCl was converted to the more thermally stable K<sub>2</sub>SO<sub>4</sub>. These findings suggest that the degree of sulphation can be estimated with the VTDMA technique, which has implications for the understanding of deposition and corrosion processes.

### 5.2.2 Effects of indirect additives

Several Several additives were tested in order to control the alkali metal flux in a DFB gasification system. The additions can be classified into direct and indirect additions, where additives are injected to the gasifier and the combustor, respectively. Direct additions can potentially have a major effect on the gas quality and imply a higher operational risk. Indirect additions tend to be less dramatic and consequently direct additions were performed at the research gasifier at Chalmers (Paper III), while the indirect effects were investigated at GoBiGas (Paper II) except in the case of S which was added indirectly in both facilities. The combined results are valuable for elucidating how the alkali metals behave in the complex DFB gasification systems. The high SID time resolution (1 s) enables time resolved characterization of the alkali metal concentration during transient conditions. For clarity, some of the results are averaged over 1 min.

The effect of indirect additions of olivine, filter ash, S and K<sub>2</sub>CO<sub>3</sub> on the product gas composition was investigated at GoBiGas (Paper II). Time series for alkali and particle concentrations are presented in Figure 23, along with the CH<sub>4</sub> concentration that is used as a proxy for tar levels. Short additions were performed to the combustor during steady-state operation, except in the case of K<sub>2</sub>CO<sub>3</sub>, which was continuously added. Elemental sulfur was

added to the combustor at two different rates, initially at a low rate, and subsequently at a higher injection rate. Note that the  $K_2CO_3$  addition was also increased when S was added (due to operation security), which means that part of the observations may originate from a higher alkali dosing, or represent a combined effect. However, during the intensified S addition, no other parameter was changed. The addition of S influences the methane concentration, while effects on alkali and particle concentrations are less apparent. Previous research suggested that  $SO_2$  may react with alkali metals in the flue gas to form solid alkali sulfate<sup>40, 95-96</sup>, which can be transferred with the bed material and enter the gasifier.<sup>12</sup> Marinkovich et al. investigated the effect of S additions during similar conditions, and suggested that  $K_2SO_4$  is possibly converted into  $K_2CO_3$  and KOH via redox reactions in the reducing environment.<sup>12</sup> This hypothesis is supported by direct additions of  $K_2SO_4$ , described below, in which an increased alkali metal concentration appeared in the product gas. However, the effect is not visible in the GoBiGas experiments, and the details of the alkali gas phase release remain unclear. The significant decrease in  $CH_4$  suggests an increased catalytic activity in the gasifier, which agrees with earlier observations.<sup>9, 12</sup> Furthermore, the question whether the increased conversion is associated with the primary pyrolysis or the secondary reforming reactions cannot be answered from these observations.

Results from additions of olivine and filter ash collected from the product gas are presented in Figure 23. Regarding olivine, the addition results in an increased  $CH_4$  concentration assigned to the lower catalytic ability of fresh olivine particles, which needs time to build an active surface layer. However, it is not yet clear why the decrease in alkali concentration is delayed with respect to the olivine addition.

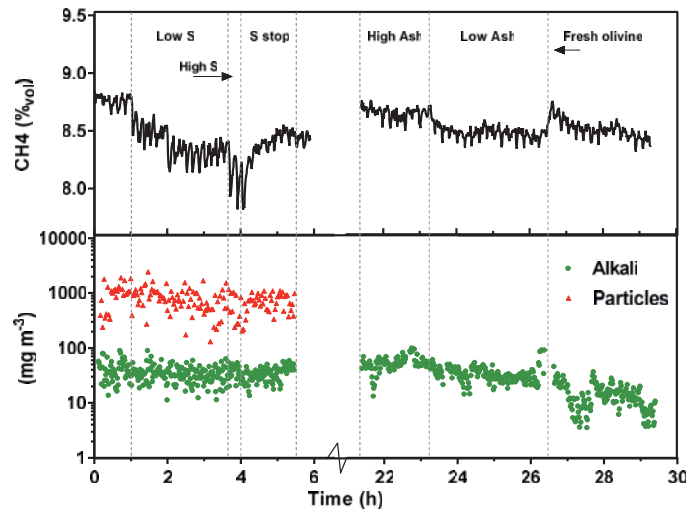


**Figure 23.** Time profile of alkali metals, particles and CH<sub>4</sub>, during addition of S, filter ash, and olivine, performed at the GoBiGas gasifier.

Regarding the recirculation of ash, the results clearly show an increased alkali metal concentration in the product gas. Note that the K<sub>2</sub>CO<sub>3</sub> addition was five times higher during the episode with low ash re-circulation, which suggests that the difference between the two ash re-circulation levels should be larger than what is visible in the obtained data. Intriguingly, the increased alkali metal concentration experienced at the higher ash recirculation does not contribute to lower tar concentrations. In contrast, the episode with low ash re-circulation and high K<sub>2</sub>CO<sub>3</sub> addition, resulted in lower CH<sub>4</sub> and alkali metal concentrations. These results suggest that the type of alkali metal, and how it interacts with the biomass, are important factors for the increased conversion.

Regarding K<sub>2</sub>CO<sub>3</sub>, it is frequently pointed out as one of the recommended additives.<sup>54, 97</sup> The catalytic effect is confirmed from previous studies and discussed in Chapter 2 of this thesis. However, much of the detailed studies have been performed in laboratory setups and some of the questions including interactions with bed material are not fully explained. For example, the partitioning between gas and liquid/solid phase in the different reactors is estimated from equilibrium calculations and only a few experimental studies from industrial scale facilities exist.<sup>92</sup>

The alkali metal measurements during the start-up sequence of GoBiGas shown in Figure 24 illuminates some of the aspects of this question. During the measurements  $K_2CO_3$  was added for 10 min at the start of every h. During these episodes an elevated concentration was observed in the product gas, meaning that potassium was transferred from the combustor and subsequently released in the gasifier during inert conditions. These findings confirm the hypothesis that olivine can be enriched with alkali metals in the combustor<sup>12, 98</sup>, which is subsequently released in the gasifier. In addition, it shows that this process is active during inert conditions in the gasifier. The drastic increase when the fuel feed started suggests that the alkali metal vapor pressure is increased in the reducing environment.

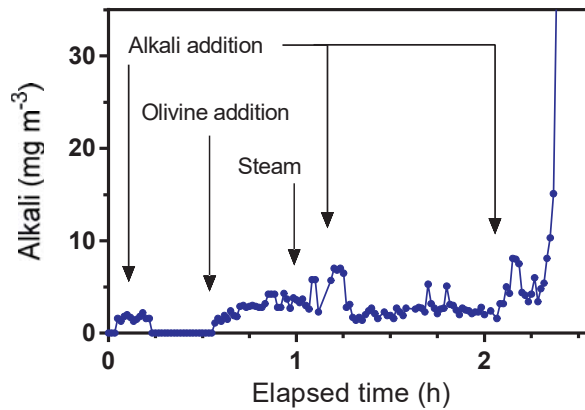


**Figure 24.** Alkali concentrations prior to fuel feeding and during start-up in the GoBiGas reactor. Alkali was added for 10 min every hour (as indicated by arrows). New bed material (olivine) was added between 0.5 h and 1.0 h. Steam fluidization started at 1.0 h and fuel feeding started at 2.3 h.

### 5.2.3 Effect of additives directly to the gasifier

Results from experiments where additions of  $K_2CO_3$  and  $K_2SO_4$  were made directly to the gasifier are presented in Figure 25 (Paper III). Salt additions resulted in a steep increase in alkali concentration indicating that decomposition and evaporation of the alkali components occur rapidly. Earlier equilibrium calculations showed possible decomposition of  $K_2SO_4(s)$  to form  $K_2CO_3(s)$  and  $KOH(g)$  under the conditions that prevail in the gasifier, as discussed

above.<sup>12, 92</sup> The  $K_2CO_3$  addition may increase the gas phase alkali metal concentration in a similar way, although it cannot be concluded from the present data. The observations from direct additions of alkali salts suggest rapid volatilization, even for the relatively stable sulfate.

Furthermore, experiments with ilmenite additions to the Chalmers gasifier operating with silica sand were performed (Paper III). The addition of ilmenite causes a significant decrease in the alkali concentration, as seen in Figure 25. Earlier research suggests that K reacts with ilmenite to form  $KTi_8O_{16}$ .<sup>14</sup> The results presented here suggests that the alkali metal uptake process is fast and efficient under steam gasification conditions. It should be pointed out that ilmenite has a catalytic effect on the tar conversion that may contribute to tar reforming and potential dilution effects, caused by the increased gas yield.<sup>13</sup> The tar interactions with minerals and alkali metals are discussed in further detail below.

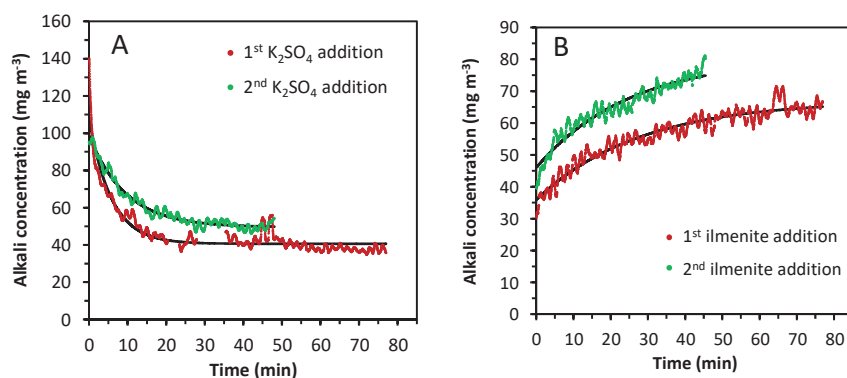


**Figure 25.** Time profile of the alkali concentration during: (A) Two additions of  $K_2SO_4$  to an olivine bed. (B) Two ilmenite additions to a silica sand bed. The end of each preceding ilmenite or  $K_2SO_4$  injection to the gasifier is set to time zero.

### 5.3 Alkali metal and tar chemistry

The observed correlations between alkali metal and tar concentrations during experiments at the Chalmers gasifier are summarized in Figure 26 (Paper III). During operation using silica sand, the observed heavy tar concentration is anti-correlated with the alkali metal concentration. The trend is further emphasized when data for higher steam flow rates of 220

and 280 kg h<sup>-1</sup> are taken into consideration. However, the results obtained using olivine as bed material do not follow the same trend. The indirect additions of S performed when the olivine bed was used may contribute to the discrepancy, but other explanations are also possible and further systematic measurements are required to thoroughly characterize the correlations.

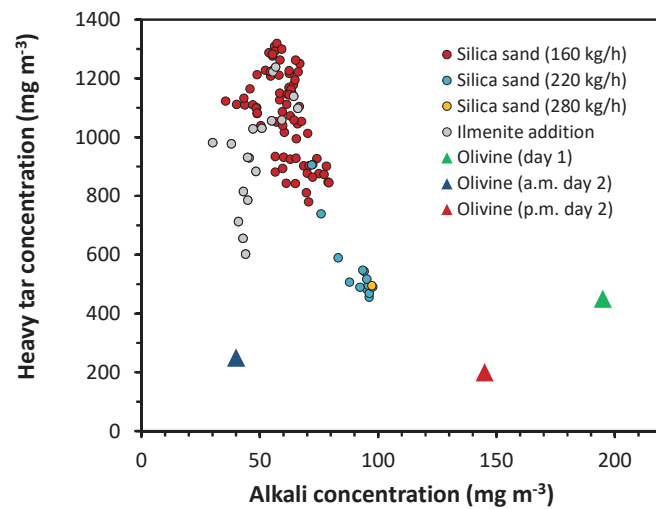


**Figure 26.** Correlation between the concentrations of heavy tar compounds and alkali metals during biomass gasification using sand and olivine as bed materials. The steam flow rates used during the silica sand experiments are indicated in the panel, and the flow rate during the olivine experiments was 160 kg h<sup>-1</sup>. Data marked “Ilmenite addition” were taken during the ongoing addition of ilmenite to the silica sand bed.

## 6. Conclusions

This thesis describes novel measurement methods for extraction and characterization of alkali metals, tar and particles in biomass thermochemical conversion. Long-term measurements were achieved by a combination of different diluters, allowing the condensable components to nucleate into aerosol particles. It is shown that the adapted techniques presented in this work can be applied in the harsh environment encountered in biomass conversion facilities. The extraction, conditioning and dilution section should be designed carefully, in order to obtain reliable long-term measurements. This section was gradually improved for the duration of this work, and the long-term measurements described at GoBiGas and the Chalmers gasifier are results of the successful progress.

The opportunity to evaluate the measurement system at the Chalmers gasifier and GoBiGas, made it possible to broaden the scope of this work. Alkali metal measurement during the commissioning of GoBiGas provided important proof-of-concept for the measurement techniques, but also interesting data showing the influence of operation conditions and the effects of different additives. The research gasifier at Chalmers on the other hand, opened up possibilities for various of additives directly to the gasifier, and the effect on product gas composition was observed.

From these measurements it can be concluded that alkali metals can be adsorbed to olivine particles under oxidizing conditions, and subsequently liberated during reducing conditions. Furthermore, the quantification suggest that high levels of alkali metals are present in a DFB steam gasifier. The direct additions of  $K_2CO_3$  and  $K_2SO_4$  to the gasifier clearly showed increased levels of alkali metals in the gas phase, suggesting that these salts rapidly volatilize at 820 °C under reducing conditions. The present data does not elucidate the detailed route for the alkali compounds in the gasifier, which is an aspect worthy of further studies. A significant reduction of the alkali vapor pressure was observed during additions of ilmenite, suggesting that the initial reaction occurs on the time scale of a few minutes. When silica sand was used as bed material, an anti-correlation between alkali metal and heavy tar concentration was observed, while no clear trend was observed when using olivine as bed material.

In summary, the measurement system provides useful data on two of the key impurities in the product gas, and the high time resolution may be important, in particular for research and commissioning applications.

Looking ahead there are some interesting experiments that can be performed to shed light on some of the unanswered questions. The VTDMA technique can be combined with mass spectrometry to give detailed molecular insight on the thermal decomposition for some of the key components in biomass gasification. The described FR-SID technique, is yet to be evaluated on product gas. A combination of thermal analysis and FR-SID would enable online characterization that can discriminate between Na and K as well as the different anions. Moreover, the laboratory experiments can easily be performed under different gas compositions. Results from such measurements are useful to understand and to control the alkali flux within a DFB system. Furthermore, experiments to prove whether the catalytic effect of potassium compounds are strongest in gas- or liquid/solid-phase would be valuable in order to further optimize the catalytic activity in the conversion process.

## Acknowledgement

I'm truly thankful to all friendly people who helped me during this work, and I would like to extend my gratitude to all of you that contribute to our open and equal society where we are privileged with a free educational system.

I would like to thank my love and best friend Marie for being a truly wonderful person and for supporting me throughout this work. A big thank you to my parents Birgitta and Jair, my brothers Michael and Jonathan for support and love.

I would like to thank my supervisor Jan Pettersson for giving me the opportunity to work and study in the interesting field of energy research and sharing knowledge and wisdom, my examiner Johan Boman for all support throughout the years, my co-supervisor Kent Davidsson for skillful assistance and clever comments on my work.

This work has involved countless hours of practical work and the following persons are gratefully acknowledged: Mohit Pushp thank you for Indian wisdom and for honest and fierce discussions, Torbjörn Gustafsson for making the delicate work of setting up a mass spec look easy, Benny Lönn for impressive construction work, Leif Holmlid and Evert Ljungström for helpful discussions.

I have had the opportunity to co-supervise following students who all made important contributions to my research: Camilla Forsman, Christina Säter, Frida Almqvist, Cecilia Öhrn and Charlotta Neiman, many thanks to all of you!

To all colleagues and friends at the Atmospheric Science Division: Mwaniki, Julia, Kong, Anna, Ågot, Pei, Dimitri, Nondas, Sofia, Michael, Christian, Josip, Erik, Ravi, Patrik and Mattias, and also former members; Cameron, Andreas, Eva, Magda, Panos and many more, thank you for a great time during coffee break, lunch, afterwork and other activities. Lots of good memories, thank you!

To members of Chalmers University Energy Technology, Martin Seemann, Anton Larsson, Johannes Öhlin, Rustan Hvitt, Jessica Bohwalli, Jelena Maric, Teresa Berdugo Vilches, Huong Nguyen, Mikael Israelsson, and Henrik Thunman, Thank you for a great cooperation! I learned a lot from working with you.

The Oxy-fuel team, Daniel Bäckström, Thomas Allgurén, Robert Johansson and Klas Andersson, many thanks for a productive cooperation and good times during the measurements.

To members of the Swedish Gasification Centre for inspiring discussions and enjoyable dinners during the conferences, Pavleta Knutsson, Michael Strand, Mario Morgalla, Placid Tchoffor, Fredrik Weiland, and many more, thank you!

Personal at Göteborg Energi and Valmet are gratefully acknowledged for the two measurement campaigns at GoBiGas, Emma Gustafsson, Claes Bretiholtz and Malin Hedenskog, thank you for all the help with setting up the measurement system and for two exciting weeks.

The five years as a PhD-student has also involved several hours of teaching, and I am grateful to: Barbara Casari, Zareen Abbas, Anders Lennartson, Lennart Sjölin, and all other lectures that made the teaching duties enjoyable. And to all students that came across my way and asked clever questions, thank you!

Other important contributions which were highly appreciated: Mikael Jansson for the Rancilio espresso machine (very useful when writing a thesis), Soheil Zackeri for Bianchi rides when you need to rest your mind from work, Tomas Bengtsson for coffee roasting et al., Martas Café (including the owner who unfortunately cannot read) for work space and company, Edmond Che Ngenhevu for early days of particle measurements.

And finally, to you, the reader, that for whatever reason are reading my thesis, thank you for your interest!

Now, on to new adventures!

A handwritten signature in black ink, appearing to read 'Dan Gall', written on a light-colored background.

Dan Gall

January 2018, Gothenburg, Sweden.



The Atmospheric Science Group. March 27<sup>th</sup> 2017, Jonsöeren. Standing from left: Yujue Wang, Michael Le Breton, Erik Thomson, Mattias Hallquist, Sofia Johansson, Samuel Mwaniki Gaita, Dan Gall, Xiangyao Pei. Seated from left: Johan Boman, Anna Lutz, Jan Pettersson, Ravi Kant Pathak. (Photo courtesy of Johan Boman).

## References

1. Pachauri, R. K.; Meyer, L. A. *IPCC: Climate Change 2014: Synthesis Report. Contribution of Working Groups I, II and III to the Fifth Assessment Report of the Intergovernmental Panel on Climate Change*; **2014**.
2. IEA. *Technology Roadmap Biofuels for Transport*; **2011**.
3. WEC. *Bioenergy - World Energy Resources*; **2016**.
4. Heidenreich, S.; Foscolo, P. U., New concepts in biomass gasification. *Progress in Energy and Combustion Science* **2015**, *46*, 72-95.
5. Bentsen, N. S.; Felby, C., Biomass for energy in the European Union - a review of bioenergy resource assessments. *Biotechnology for Biofuels* **2012**, *5*, 25.
6. O'Brien, M.; Wechsler, D.; Bringezu, S.; Schaldach, R., Toward a systemic monitoring of the European bioeconomy: Gaps, needs and the integration of sustainability indicators and targets for global land use. *Land Use Policy* **2017**, *66*, 162-171.
7. Bond, T. C.; Streets, D. G.; Yarber, K. F.; Nelson, S. M.; Woo, J. H.; Klimont, Z., A technology-based global inventory of black and organic carbon emissions from combustion. *Journal of Geophysical Research-Atmospheres* **2004**, *109*, 43.
8. Laden, F.; Neas, L. M.; Dockery, D. W.; Schwartz, J., Association of fine particulate matter from different sources with daily mortality in six US cities. *Environ. Health Perspect.* **2000**, *108*, 941-947.
9. Alamia, A.; Larsson, A.; Breitholtz, C.; Thunman, H., Performance of large-scale biomass gasifiers in a biorefinery, a state-of-the-art reference. *International Journal of Energy Research* **2017**, *14*, 2001-2019.
10. Elliot, D., A balancing act for renewables. *Nature Energy* **2016**, *1*.
11. Devi, L.; Ptasiński, K. J.; Janssen, F. J. J. G., A review of the primary measures for tar elimination in biomass gasification processes. *Biomass and Bioenergy* **2003**, *24*, 125-140.
12. Marinkovic, J.; Thunman, H.; Knutsson, P.; Seemann, M., Characteristics of olivine as a bed material in an indirect biomass gasifier. *Chem. Eng. J.* **2015**, *279*, 555-566.
13. Lind, F.; Berguerand, N.; Seemann, M.; Thunman, H., Ilmenite and Nickel as Catalysts for Upgrading of Raw Gas Derived from Biomass Gasification. *Energy & Fuels* **2013**, *27*, 997-1007.
14. Corcoran, A.; Marinkovic, J.; Lind, F.; Thunman, H.; Knutsson, P.; Seemann, M., Ash Properties of Ilmenite Used as Bed Material for Combustion of Biomass in a Circulating Fluidized Bed Boiler. *Energy & Fuels* **2014**, *28*, 7672-7679.

15. Devi, L.; Craje, M.; Thune, P.; Ptasinski, K. J.; Janssen, F., Olivine as tar removal catalyst for biomass gasifiers: Catalyst characterization. *Applied Catalysis a-General* **2005**, *294*, 68-79.
16. He, H. B.; Skoglund, N.; Ohman, M., Time-Dependent Crack Layer Formation in Quartz Bed Particles during Fluidized Bed Combustion of Woody Biomass. *Energy & Fuels* **2017**, *31*, 1672-1677.
17. Kirnbauer, F.; Hofbauer, H., The mechanism of bed material coating in dual fluidized bed biomass steam gasification plants and its impact on plant optimization. *Powder Technology* **2013**, *245*, 94-104.
18. Kuba, M.; He, H. B.; Kirnbauer, F.; Skoglund, N.; Bostrom, D.; Ohman, M.; Hofbauer, H., Mechanism of Layer Formation on Olivine Bed Particles in Industrial-Scale Dual Fluid Bed Gasification of Wood. *Energy & Fuels* **2016**, *30*, 7410-7418.
19. van Paasen, J. P. A.; Devi, L.; Janssen, F.; Meijer, R.; Berends, H. M. G.; Temmink, G.; Padban, E. A. *Primary measures to reduce tar format ion in fluidised-bed biomass gasifiers*; 2004.
20. Carpenter, D. L.; Deutch, S. P.; French, R. J., Quantitative measurement of Biomass gasifier tars using a molecular-beam mass spectrometer: Comparison with traditional impinger sampling. *Energy & Fuels* **2007**, *21*, 3036-3043.
21. Horvat, A.; Kwapinska, M.; Xue, G.; Dooley, S.; Kwapinski, W.; Leahy, J. J., Detailed Measurement Uncertainty Analysis of Solid-Phase Adsorption-Total Gas Chromatography (GC)-Detectable Tar from Biomass Gasification. *Energy & Fuels* **2016**, *30*, 2187-2197.
22. Brage, C.; Yu, Q. Z.; Chen, G. X.; Sjoström, K., Use of amino phase adsorbent for biomass tar sampling and separation. *Fuel* **1997**, *76*, 137-142.
23. Neubert, M.; Reil, S.; Wolff, M.; Pocher, D.; Stork, H.; Ultsch, C.; Meiler, M.; Messer, J.; Kinzler, L.; Dillig, M.; Beer, S.; Karl, J., Experimental comparison of solid phase adsorption (SPA), activated carbon test tubes and tar protocol (DIN CEN/TS 15439) for tar analysis of biomass derived syngas. *Biomass Bioenerg.* **2017**, *105*, 443-452.
24. Sun, R. H.; Zobel, N.; Neubauer, Y.; Chavez, C. C.; Behrendt, F., Analysis of gas-phase polycyclic aromatic hydrocarbon mixtures by laser-induced fluorescence. *Opt. Lasers Eng.* **2010**, *48*, 1231-1237.
25. Erbel, C.; Mayerhofer, M.; Monkhouse, P.; Gaderer, M.; Spliethoff, H., Continuous in situ measurements of alkali species in the gasification of biomass. *Proc. Combust. Inst.* **2013**, *34*, 2331-2338.
26. Karellas, S.; Karl, J., Analysis of the product gas from biomass gasification by means of laser spectroscopy. *Opt. Lasers Eng.* **2007**, *45*, 935-946.
27. Carpenter, D. L. In *Molecular Beam Mass Spectrometry for Analysis of Condensable Gas Components*, 19th EU Biomass Conference Berlin, Berlin, 2011.

28. Dufour, A.; Girods, P.; Masson, E.; Normand, S.; Rogaume, Y.; Zoulalian, A., Comparison of two methods of measuring wood pyrolysis tar. *Journal of Chromatography A* **2007**, *1164*, 240-247.
29. Defoort, F.; Thiery, S.; Ravel, S., A promising new on-line method of tar quantification by mass spectrometry during steam gasification of biomass. *Biomass Bioenerg.* **2014**, *65*, 64-71.
30. Ahmadi, M.; Knoef, H.; Van de Beld, B.; Liliedahl, T.; Engvall, K., Development of a PID based on-line tar measurement method - Proof of concept. *Fuel* **2013**, *113*, 113-121.
31. Rechulski, M. D. K.; Schneebeil, J.; Geiger, S.; Schildhauer, T. J.; Biollaz, S. M. A.; Ludwig, C., Liquid-Quench Sampling System for the Analysis of Gas Streams from Biomass Gasification Processes. Part 2: Sampling Condensable Compounds. *Energy & Fuels* **2012**, *26*, 6358-6365.
32. Edinger, P.; Schneebeil, J.; Struis, R.; Biollaz, S. M. A.; Ludwig, C., On-line liquid quench sampling and UV-Vis spectroscopy for tar measurements in wood gasification process gases. *Fuel* **2016**, *184*, 59-68.
33. Israelsson, M.; Larsson, A.; Thunman, H., Online Measurement of Elemental Yields, Oxygen Transport, Condensable Compounds, and Heating Values in Gasification Systems. *Energy & Fuels* **2014**, *28*, 5892-5901.
34. Vassilev, S. V.; Baxter, D.; Andersen, L. K.; Vassileva, C. G., An overview of the chemical composition of biomass. *Fuel* **2010**, *89*, 913-933.
35. Vassilev, S. V.; Baxter, D.; Andersen, L. K.; Vassileva, C. G., An overview of the composition and application of biomass ash. Part 1. Phase-mineral and chemical composition and classification. *Fuel* **2013**, *105*, 40-76.
36. Olsson, J. G.; Jäglid, U.; Pettersson, J. B. C.; Hald, P., Alkali Metal Emission during Pyrolysis of Biomass. *Energy & Fuels* **1997**, *11*, 779-784.
37. Tchoffor, P. A.; Davidsson, K. O.; Thunman, H., Transformation and Release of Potassium, Chlorine, and Sulfur from Wheat Straw under Conditions Relevant to Dual Fluidized Bed Gasification. *Energy & Fuels* **2013**, *27*, 7510-7520.
38. Tchoffor, P. A.; Moradian, F.; Pettersson, A.; Davidsson, K. O.; Thunman, H., Influence of Fuel Ash Characteristics on the Release of Potassium, Chlorine, and Sulfur from Biomass Fuels under Steam-Fluidized Bed Gasification Conditions. *Energy & Fuels* **2016**, *30*, 10435-10442.
39. Sepman, A.; Ögren, Y.; Qu, Z.; Wiinikka, H.; Schmidt, F. M., Real-time in situ multi-parameter TDLAS sensing in the reactor core of an entrained-flow biomass gasifier. *Proc. Combust. Inst.* **2017**, *36*, 4541-4548.
40. Zhang, Z.; Liu, J.; Shen, F. H.; Yang, Y. J.; Liu, F., On-line measurement and kinetic studies of sodium release during biomass gasification and pyrolysis. *Fuel* **2016**, *178*, 202-208.
41. Porbatzki, D.; Stemmler, M.; Muller, M., Release of inorganic trace elements during gasification of wood, straw, and miscanthus. *Biomass Bioenerg.* **2011**, *35*, S79-S86.

42. Olsson, J. G.; Pettersson, J. B. C.; Padban, N.; Bjerle, I., Alkali Metal Emission from Filter Ash and Fluidized Bed Material from PFB Gasification of Biomass. *Energy & Fuels* **1998**, *12*, 626-630.
43. Kowalski, T.; Ludwig, C.; Wokaun, A., Qualitative Evaluation of Alkali Release during the Pyrolysis of Biomass. *Energy & Fuels* **2007**, *21*, 3017-3022.
44. Wellinger, M.; Biollaz, S.; Wochele, J.; Ludwig, C., Sampling and Online Analysis of Alkalies in Thermal Process Gases with a Novel Surface Ionization Detector. *Energy & Fuels* **2011**, *25*, 4163-4171.
45. Knutsson, P.; Lai, H.; Stiller, K., A method for investigation of hot corrosion by gaseous Na<sub>2</sub>SO<sub>4</sub>. *Corrosion Science* **2013**, *73*, 230-236.
46. Larsson, E.; Gruber, H.; Hellstrom, K.; Jonsson, T.; Liske, J.; Svensson, J. E., A Comparative Study of the Initial Corrosion of KCl and PbCl<sub>2</sub> on a Low-Alloyed Steel. *Oxid. Met.* **2017**, *87*, 779-787.
47. Sekiguchi, Y.; Shafizadeh, F., The effect of inorganic additives on the formation, composition, and combustion of cellulosic char. *J. Appl. Polym. Sci.* **1984**, *29*, 1267-1286.
48. Patwardhan, P. R.; Satrio, J. A.; Brown, R. C.; Shanks, B. H., Influence of inorganic salts on the primary pyrolysis products of cellulose. *Bioresour. Technol.* **2010**, *101*, 4646-4655.
49. Wang, S. R.; Liu, Q.; Liao, Y. F.; Luo, Z. Y.; Cen, K. F., A study on the mechanism research on cellulose pyrolysis under catalysis of metallic salts. *Korean Journal of Chemical Engineering* **2007**, *24*, 336-340.
50. Piskorz, J.; Radlein, D.; Scott, D. S., On the mechanism of the rapid pyrolysis of cellulose. *J. Anal. Appl. Pyrolysis* **1986**, *9*, 121-137.
51. Richards, G. N., Glycolaldehyde from pyrolysis of cellulose. *J. Anal. Appl. Pyrolysis* **1987**, *10*, 251-255.
52. Patwardhan, P. R.; Satrio, J. A.; Brown, R. C.; Shanks, B. H., Product distribution from fast pyrolysis of glucose-based carbohydrates. *J. Anal. Appl. Pyrolysis* **2009**, *86*, 323-330.
53. Yang, C. Y.; Lu, X. S.; Lin, W. G.; Yang, X. M.; Yao, J. Z., TG-FTIR study on corn straw pyrolysis-influence of minerals. *Chem. Res. Chin. Univ.* **2006**, *22*, 524-532.
54. Sutton, D.; Kelleher, B.; Ross, J. R. H., Review of literature on catalysts for biomass gasification. *Fuel Processing Technology* **2001**, *73*, 155-173.
55. Kirnbauer, F.; Wilk, V.; Kitzler, H.; Kern, S.; Hofbauer, H., The positive effects of bed material coating on tar reduction in a dual fluidized bed gasifier. *Fuel* **2012**, *95*, 553-562.
56. Giechaskiel, B.; Ntziachristos, L.; Samaras, Z., Effect of ejector dilutors on measurements of automotive exhaust gas aerosol size distributions. *Meas. Sci. Technol.* **2009**, *20*, 7.

57. Lipsky, E. M.; Robinson, A. L., Effects of dilution on fine particle mass and partitioning of semivolatile organics in diesel exhaust and wood smoke. *Environ. Sci. Technol.* **2006**, *40*, 155-162.
58. Jensen, J. R.; Nielsen, L. B.; Schultz-Moller, C.; Wedel, S.; Livbjerg, H., The nucleation of aerosols in flue gases with a high content of alkali - A laboratory study. *Aerosol Science and Technology* **2000**, *33*, 490-509.
59. Pankow, J. F., Review and comparative-analysis of the theories on partitioning between the gas and aerosol particulate phases in the atmosphere. *Atmospheric Environment* **1987**, *21*, 2275-2283.
60. Knutson, E. O.; Whitby, K. T., Aerosol classification by electric mobility: apparatus, theory, and applications. *Journal of Aerosol Science* **1975**, *6*, 443-451.
61. Hinds, W., *Aerosol technology*. 2nd ed.; John Wiley & Sons, inc.: **1999**.
62. Sousan, S.; Koehler, K.; Hallett, L.; Peters, T. M., Evaluation of the Alphasense optical particle counter (OPC-N2) and the Grimm portable aerosol spectrometer (PAS-1.108). *Aerosol Science and Technology* **2016**, *50*, 1352-1365.
63. Dinoi, A.; Donato, A.; Belosi, F.; Conte, M.; Contini, D., Comparison of atmospheric particle concentration measurements using different optical detectors: Potentiality and limits for air quality applications. *Measurement* **2017**, *106*, 274-282.
64. Vyazovkin, S., Thermogravimetric Analysis. In *Characterization of Materials*, John Wiley & Sons, Inc.: **2002**.
65. Salo, K.; Jonsson, A. M.; Andersson, P. U.; Hallquist, M., Aerosol Volatility and Enthalpy of Sublimation of Carboxylic Acids. *Journal of Physical Chemistry A* **2010**, *114*, 4586-4594.
66. Hallquist, A. M.; Fridell, E.; Westerlund, J.; Hallquist, M., Onboard Measurements of Nanoparticles from a SCR-Equipped Marine Diesel Engine. *Environmental Science and Technology* **2013**, *47*, 773-780.
67. Jonsson, A. M.; Hallquist, M.; Saathoff, H., Volatility of secondary organic aerosols from the ozone initiated oxidation of alpha-pinene and limonene. *Journal of Aerosol Science* **2007**, *38*, 843-852.
68. Emanuelsson, E. U.; Watne, A. K.; Lutz, A.; Ljungstrom, E.; Hallquist, M., Influence of Humidity, Temperature, and Radicals on the Formation and Thermal Properties of Secondary Organic Aerosol (SOA) from Ozonolysis of beta-Pinene. *Journal of Physical Chemistry A* **2013**, *117*, 10346-10358.
69. Villani, P.; Picard, D.; Marchand, N.; Laj, P., Design and validation of a 6-volatility tandem differential mobility analyzer (VTDMA). *Aerosol Science and Technology* **2007**, *41*, 898-906.
70. Philippin, S.; Wiedensohler, A.; Stratmann, F., Measurements of non-volatile fractions of pollution aerosols with an eight-tube volatility tandem differential mobility analyzer (VTDMA-8). *Journal of Aerosol Science* **2004**, *35*, 185-203.

71. Bilde, M.; Pandis, S. N., Evaporation rates and vapor pressures of individual aerosol species formed in the atmospheric oxidation of  $\alpha$ - and  $\beta$ - pinene. *Environmental Science and Technology* **2001**, *35*, 3344-3349.
72. Bird, R. B.; Stewart, W. E.; Lightfoot, E. N., *Transport Phenomena*. John Wiley & Sons, Inc: New York, **2002**.
73. Fuchs, N. A.; Sutugin, A. G., Topics in Current Aerosol Research. **1971**.
74. Julin, J.; Winkler, P. M.; Donahue, N. M.; Wagner, P. E.; Riipinen, I., Near-Unity Mass Accommodation Coefficient of Organic Molecules of Varying Structure. *Environmental Science and Technology* **2014**, *48*, 12083-12089.
75. Fuentes, E.; McFiggans, G., A modeling approach to evaluate the uncertainty in estimating the evaporation behaviour and volatility of organic aerosols. *Atmospheric Measurement Techniques* **2012**, *5*, 735-757.
76. Davidsson, K. O.; Engvall, K.; Hagstrom, M.; Korsgren, J. G.; Lonn, B.; Pettersson, J. B. C., A surface ionization instrument for on-line measurements of alkali metal components in combustion: Instrument description and applications. *Energy & Fuels* **2002**, *16*, 1369-1377.
77. Jaglid, U.; Olsson, J. G.; Pettersson, J. B. C., Detection of sodium and potassium salt particles using surface ionization at atmospheric pressure. *Journal of Aerosol Science* **1996**, *27*, 967-977.
78. Svane, M.; Gustafsson, T. L.; Kovacevik, B.; Noda, J.; Andersson, P. U.; Nilsson, E. D.; Pettersson, J. B. C., On-Line Chemical Analysis of Individual Alkali-Containing Aerosol Particles by Surface Ionization Combined with Time-of-Flight Mass Spectrometry. *Aerosol Science and Technology* **2009**, *43*, 653-661.
79. Svane, M.; Hagstrom, M.; Pettersson, J. B. C., Online measurements of individual alkali-containing particles formed in biomass and coal combustion: Demonstration of an instrument based on surface ionization technique. *Energy & Fuels* **2005**, *19*, 411-417.
80. Hagstrom, M.; Engvall, K.; Pettersson, J. B. C., Desorption kinetics at atmospheric pressure: Alkali metal ion emission from hot platinum surfaces. *Journal of Physical Chemistry B* **2000**, *104*, 4457-4462.
81. Holmlid, L.; Olsson, J. O., Simple surface ionization detector with field reversal for absolute ionization coefficient and ionic and neutral desorption measurements. *Rev. Sci. Instrum.* **1976**, *47*, 1167-1171.
82. Kaminsky, M., *Atomic and Ionic impact phenomena on metal surfaces*. Academic Press Inc. : **1965**.
83. TSI Inc. *Measuring nanoparticle size distributions in real-time: Key factors for accuracy*; **2012**.
84. McMurry, P. H., A review of atmospheric aerosol measurements. *Atmospheric Environment* **2000**, *34*, 1959-1999.

85. Buonanno, G.; Dell'Isola, M.; Stabile, L.; Viola, A., Uncertainty Budget of the SMPS–APS System in the Measurement of PM<sub>1</sub>, PM<sub>2.5</sub>, and PM<sub>10</sub>. *Aerosol Science and Technology* **2009**, *43*, 1130-1141.
86. Burkart, J.; Steiner, G.; Reischl, G.; Moshhammer, H.; Neuberger, M.; Hitznerberger, R., Characterizing the performance of two optical particle counters (Grimm OPC1.108 and OPC1.109) under urban aerosol conditions. *Journal of Aerosol Science* **2010**, *41*, 953-962.
87. JCGM *Evaluation of measurement data — Guide to the expression of uncertainty in measurement* **2008**.
88. Thunman, H.; Seemann, M. C., First Experiences with the New Chalmers Gasifier. In *Proceedings of the 20th International Conference on Fluidized Bed Combustion*, Yue, G.; Zhang, H.; Zhao, C.; Luo, Z., Eds. Springer Berlin Heidelberg: 2010; pp 659-663.
89. Andersson, K.; Johnsson, F., Flame and radiation characteristics of gas-fired O<sub>2</sub>/CO<sub>2</sub> combustion. *Fuel* **2007**, *86*, 656-668.
90. Rys, M. Investigation of Thermodynamic Properties of Alkali Metals in Oxide Systems Relevant to Coal Slags. Aachen University, **2007**.
91. Lau, K. H. C., D.; Hildenbrand, D. L., Effusion Studies of the Vaporization/Decomposition of Potassium Sulfate. *Journal of The Electrochemical Society* **1979**, 490-495.
92. Norheim, A.; Lindberg, D.; Hustad, J. E.; Backman, R., Equilibrium Calculations of the Composition of Trace Compounds from Biomass Gasification in the Solid Oxide Fuel Cell Operating Temperature Interval. *Energy & Fuels* **2009**, *23*, 920-925.
93. Lehman, R. L.; Gentry, J. S.; Glumac, N. G., Thermal stability of potassium carbonate near its melting point. *Thermochimica Acta* **1998**, *316*, 1-9.
94. Higgins, K. J.; Jung, H. J.; Kittelson, D. B.; Roberts, J. T.; Zachariah, M. R., Size-selected nanoparticle chemistry: Kinetics of soot oxidation. *Journal of Physical Chemistry A* **2002**, *106*, 96-103.
95. Glarborg, P.; Marshall, P., Mechanism and modeling of the formation of gaseous alkali sulfates. *Combustion and Flame* **2005**, *141*, 22-39.
96. Jin, X.; Ye, J. M.; Deng, L.; Che, D. F., Condensation Behaviors of Potassium during Biomass Combustion. *Energy & Fuels* **2017**, *31*, 2951-2958.
97. Abu El-Rub, Z.; Bramer, E. A.; Brem, G., Review of catalysts for tar elimination in Biomass gasification processes. *Industrial & Engineering Chemistry Research* **2004**, *43*, 6911-6919.
98. Kirnbauer, F.; Koch, M.; Koch, R.; Aichernig, C.; Hofbauer, H., Behavior of Inorganic Matter in a Dual Fluidized Steam Gasification Plant. *Energy & Fuels* **2013**, *27*, 3316-3331.